16. Maher SG, Sheikh F, Scarzello AJ, Romero-Weaver AL, Baker DP, Donnelly RP, et al. IFNalpha and IFNlambda differ in their antiproliferative effects and duration of JAK/STAT signaling activity. Cancer Biol Ther. 2008;7:1109–15.
17. Tateishi R, Shiina S, Teratani T, Obi S, Sato S, Koike Y, et al. Percutaneous radiofrequency ablation for hepatocellular carcinoma. An analysis of 1000 cases. Cancer. 2005;2005(103): 1201–9.
18. Masuzaki R, Tateishi R, Yoshida H, Goto E, Sato T, Ohki T, et al. Prospective risk assessment for hepatocellular carcinoma development in patients with chronic hepatitis C by transient elastography. Hepatology. 2009;49:1954–61.
19. Wai CT, Greenson JK, Fontana RJ, Kalbfleisch JD, Marrero JA, Conjeevaram HS, et al. A simple noninvasive index can predict both significant fibrosis and cirrhosis in patients with chronic hepatitis C. Hepatology. 2003;38:518–26.
20. Kiyosawa K, Umemura T, Ichijo T, Matsumoto A, Yoshizawa K, Gad A, et al. Hepatocellular carcinoma: recent trends in Japan. Gastroenterology. 2004;127:S17–26.
21. El-Serag HB, Rudolph KL. Hepatocellular carcinoma: epidemiology and molecular carcinogenesis. Gastroenterology. 2007;132: 2557–76.
22. Kumar V, Kato N, Urabe Y, Takahashi A, Muroyama R, Hosono N, et al. Genome-wide association study identifies a susceptibility locus for HCV-induced hepatocellular carcinoma. Nat Genet. 2011;43:455–8.
23. Miki D, Ochi H, Hayes CN, Abe H, Yoshima T, Aikata H, et al. Variation in the DEPDC5 locus is associated with progression to hepatocellular carcinoma in chronic hepatitis C virus carriers. Nat Genet. 2011;43:797–800.
24. McCarthy MI, Abecasis GR, Cardon LR, Goldstein DB, Little J, Ioannidis JP, et al. Genome-wide association studies for complex traits: consensus, uncertainty and challenges. Nat Rev Genet. 2008;9:356–69.
25. Cantor RM, Lange K, Sinsheimer JS. Prioritizing GWAS results: a review of statistical methods and recommendations for their application. Am J Hum Genet. 2010;86:6–22.
26. Johnson RC, Nelson GW, Troyer JL, Lautenberger JA, Kessing BD, Winkler CA, et al. Accounting for multiple comparisons in a genome-wide association study (GWAS). BMC Genomics. 2010; 11:724.
27. Asahina Y, Tanaka K, Suzuki Y, Tamaki N, Hoshioka T, Kato T, et al. Association between IL28B gene variation and development of hepatocellular carcinoma after interferon therapy in patients with chronic hepatitis C. J Hepatol. 2011;54:S37.
28. Fabris C, Falleti E, Cussigh A, Bitetto D, Fontanini E, Bignulin S, et al. IL-28B rs12979860 C/T allele distribution in patients with liver cirrhosis: role in the course of chronic viral hepatitis and the development of HCC. J Hepatol. 2011;54:716–22.
29. Bochud PY, Bibert S, Kutalik Z, Patin E, Guergnon J, Nalpas B, et al. IL28B alleles associated with poor hepatitis C virus (HCV) clearance protect against inflammation and fibrosis in patients infected with non-1 HCV genotypes. Hepatology. 2012;55:384–94.
30. Joshita S, Umemura T, Katsuyama Y, Ichikawa Y, Kimura T, Morita S, et al. Association of IL28B gene polymorphism with development of hepatocellular carcinoma in Japanese patients with chronic hepatitis C virus infection. Hum Immunol. 2012;73:298–300.
31. Miura M, Maekawa S, Kadokura M, Sueki R, Komase K, Shindo H, et al. Analysis of viral amino acids sequences and the IL28B SNP influencing the development of hepatocellular carcinoma in chronic hepatitis C. Hepatol Int. 2012;6:386–96.
32. Agundez JA, Garcia-Martin E, Maestro ML, Cuenca F, Martinez C, Ortega L, et al. Relation of IL28B gene polymorphism with biochemical and histological features in hepatitis C virus-induced liver disease. PLoS ONE. 2012;7:e37998.
33. Bruno S, Crosignani A, Maisonneuve P, Rossi S, Silini E, Mondelli MU. Hepatitis C virus genotype 1b as a major risk factor associated with hepatocellular carcinoma in patients with cirrhosis: a seventeen-year prospective cohort study. Hepatology. 2007;46:1350–6.
34. Bruno S, Silini E, Crosignani A, Borzio F, Leandro G, Bono F, et al. Hepatitis C virus genotypes and risk of hepatocellular carcinoma in cirrhosis: a prospective study. Hepatology. 1997;25: 754–8.
35. Silini E, Bottelli R, Asti M, Bruno S, Candusso ME, Brambilla S, et al. Hepatitis C virus genotypes and risk of hepatocellular carcinoma in cirrhosis: a case-control study. Gastroenterology. 1996;111:199–205.
36. Freeman AJ, Dore GJ, Law MG, Thorpe M, Von Overbeck J, Lloyd AR, et al. Estimating progression to cirrhosis in chronic hepatitis C virus infection. Hepatology. 2001;34:809–16.
37. Moghaddam A, Melum E, Reinton N, Ring-Larsen H, Verbaan H, Bjoro K, et al. IL28B genetic variation and treatment response in patients with hepatitis C virus genotype 3 infection. Hepatology. 2011;53:746–54.
38. Abe H, Ochi H, Maekawa T, Hayes CN, Tsuge M, Miki D, et al. Common variation of IL28 affects gamma-GTP levels and inflammation of the liver in chronically infected hepatitis C virus patients. J Hepatol. 2010;53:439–43.
39. Li Q, Kawamura K, Ma G, Iwata F, Numasaki M, Suzuki N, et al. Interferon-lambda induces G1 phase arrest or apoptosis in oesophageal carcinoma cells and produces anti-tumour effects in combination with anti-cancer agents. Eur J Cancer. 2010;46: 180–90.
40. Lasfar A, Lewis-Antes A, Smirnov SV, Anantha S, Abushahba W, Tian B, et al. Characterization of the mouse IFN-lambda ligand-receptor system: IFN-lambdas exhibit antitumor activity against B16 melanoma. Cancer Res. 2006;66:4468–77.
41. Abushahba W, Balan M, Castaneda I, Yuan Y, Reuhl K, Raveche E, et al. Antitumor activity of type I and type III interferons in BNL hepatoma model. Cancer Immunol Immunother. 2010;59: 1059–71.
42. Sato A, Ohtsuki M, Hata M, Kobayashi E, Murakami T. Antitumor activity of IFN-lambda in murine tumor models. J Immunol. 2006;176:7686–94.
43. Zitzmann K, Brand S, Baehs S, Goke B, Meinecke J, Spottl G, et al. Novel interferon-lambdas induce antiproliferative effects in neuroendocrine tumor cells. Biochem Biophys Res Commun. 2006;344:1334–41.
44. Khan DA, Fatima Tuz Z, Khan FA, Mubarak A. Evaluation of diagnostic accuracy of APRI for prediction of fibrosis in hepatitis C patients. J Ayub Med Coll Abbottabad. 2008;20:122–6.
45. Sebastiani G, Vario A, Guido M, Noventa F, Plebani M, Pistis R, et al. Stepwise combination algorithms of non-invasive markers to diagnose significant fibrosis in chronic hepatitis C. J Hepatol. 2006;44:686–93.

Open

CT With Hepatic Arterioportography as a Pretreatment Examination for Hepatocellular Carcinoma Patients: A Randomized Controlled Trial

Takamasa Ohki, MD, PhD[1,2,6], Ryosuke Tateishi, MD, PhD[1,6], Masaaki Akahane, MD, PhD[3], Shintaro Mikami, MD, PhD[1], Masaya Sato, MD, PhD[1], Koji Uchino, MD, PhD[1], Toru Arano, MD, PhD[1], Kenichiro Enooku, MD, PhD[1], Yuji Kondo, MD, PhD[1], Noriyo Yamashiki, MD, PhD[1], Tadashi Goto, MD, PhD[1], Shuichiro Shiina, MD, PhD[1], Haruhiko Yoshida, MD, PhD[1], Yutaka Matsuyama, PhD[4], Masao Omata, MD, PhD[5], Kuni Ohtomo, MD, PhD[3] and Kazuhiko Koike, MD, PhD[1]

OBJECTIVES: **The combination of computed tomography with hepatic arteriography and arterial portography (CTHA/CTAP) can detect additional hepatocellular carcinoma (HCC) nodules undetected by conventional dynamic CT.**

METHODS: **In this single-center, randomized, open-label, controlled trial, we randomly assigned 280 patients who were diagnosed as having HCC by conventional dynamic CT, and eligible for radiofrequency ablation (RFA), to undergo CTHA/CTAP before treatment, or to the control group. Newly detected HCC nodules by CTHA/CTAP were intended to be ablated completely. The primary end point was recurrence-free survival and the key secondary end point was overall survival. The analysis was conducted on an intention-to-treat basis. Those with nonablated nodules were treated as for recurrence.**

RESULTS: **A total of 75 nodules were newly diagnosed as HCC by CTHA/CTAP in 45 patients. Three patients (one in the CTHA/CTAP group and two in the control group) who refused treatment were excluded from all analyses. The cumulative recurrence-free survival rates at 1, 2, and 3 years were 60.1, 29.0, and 18.9% in the CTHA/CTAP group and 52.2, 29.7, and 23.1% in the control group, respectively (P=0.66 by log-rank test; hazard ratio, 0.94 for CTHA/CTAP vs. control; 95% confidence interval (CI), 0.73–1.22). The cumulative overall survival rates at 3 and 5 years were 79.7 and 56.4% in the CTHA/CTAP group and 86.8 and 60.1% in the control group, respectively (P=0.50; hazard ratio, 1.15, 95% CI, 0.77–1.71).**

CONCLUSIONS: **CTHA/CTAP may detect recurrent lesions earlier. However, CTHA/CTAP before RFA did not improve cumulative recurrence-free survival or overall survival.**

Am J Gastroenterol 2013; 108:1305–1313; doi:10.1038/ajg.2013.109; published online 30 April 2013

INTRODUCTION

Hepatocellular carcinoma (HCC) ranks as the fifth most common cancer worldwide (1). In Japan, ~35,000 patients die from HCC every year (2), and the main cause of HCC is hepatitis C virus infection. In chronic hepatitis patients, screening of HCC is usually performed by ultrasonography, and the diagnosis is confirmed by contrast-enhanced dynamic computed tomography (CT). Hyperattenuation in the arterial phase and hypoattenuation in the equilibrium phase are considered to be definitive signs of HCC (3–7). Hyperattenuation in the arterial phase is more emphasized when contrast material is injected from the hepatic artery through a catheter, because dilution of contrast material in the systemic circulation is avoided, thus keeping a high concentration of contrast material in the liver. This technique is called CT during hepatic arteriography (CTHA) (6,8–10). Similarly, hypoattenuation in the equilibrium phase is accentuated after injection of contrast material into the superior mesenteric artery, which is referred to as CT during arterial portography (CTAP) (11–14). The combination of CTHA and CTAP gives higher sensitivity and specificity for HCC detection than conventional dynamic enhanced CT (8).

[1]Department of Gastroenterology, Graduate School of Medicine, University of Tokyo, Tokyo, Japan; [2]Department of Gastroenterology, Mitsui Memorial Hospital, Tokyo, Japan; [3]Department of Radiology, Graduate School of Medicine, University of Tokyo, Tokyo, Japan; [4]Department of Biostatistics, Graduate School of Medicine, University of Tokyo, Tokyo, Japan; [5]Yamanashi Prefectural Hospital Organization, Kofu, Japan; [6]The first two authors contributed equally to this work.
Correspondence: Ryosuke Tateishi, MD, PhD, Department of Gastroenterology, Graduate School of Medicine, University of Tokyo, 7-3-1 Hongo, Bunkyo-ku, Tokyo 113-8655, Japan. E-mail: tateishi-tky@umin.ac.jp
Received 25 September 2012; accepted 12 March 2013

If new HCC nodules are detected with CTHA/CTAP, in addition to those detected with dynamic CT, the treatment of choice may be changed (15,16). For example, surgical resection and liver transplantation are usually contraindicated for multinodular HCC; that is, exceeding three nodules. Percutaneous tumor ablation methods, such as ethanol injection and microwave coagulation, have played an important role as nonsurgical treatments that can achieve high local cure rates without affecting background liver function (17–20). Radiofrequency ablation (RFA) is currently considered to be the most effective first-line percutaneous ablation protocol because of its greater efficacy in terms of local cure as compared with ethanol injection (21–24). However, even after complete ablation, patients frequently encounter intrahepatic tumor recurrence at a rate of 50% in 2 years, the majority of which occurs at locations distant from the primary ablated site (25). Considering the tumor doubling time, many nodules diagnosed as recurrent within 2 years were probably present at the time of first ablation. If nodules that are undetectable by conventional dynamic CT could be detected and ablated, the recurrence rate would be decreased.

Although CTHA/CTAP is one of the most sensitive techniques available for detection of small HCC, its disadvantages include invasiveness, high cost, and a high false-positive rate (26). The indication for CTHA/CTAP can be justified only when the expected benefits exceed the risk and cost of the procedure. We conducted a single-center, randomized, open-label, controlled trial to assess the utility of CTHA/CTAP before RFA in patients with early-stage HCC by comparing recurrence-free and overall survival.

METHODS

Patients

The study population consisted of patients with early-stage HCC with an indication for RFA. Those who met the following criteria were enrolled between September 2004 and February 2009: (i) diagnosis of typical HCC on dynamic CT performed within 2 weeks, i.e., hyperattenuation during the arterial phase and hypoattenuation during the equilibrium phase (5,6); (ii) tumor size ≤3.0 cm and no more than three tumor nodules; (iii) Child–Pugh class A liver function; and (iv) age >20 years. Exclusion criteria were: allergy to contrast media; portal or hepatic vein tumor thrombosis; extrahepatic metastasis; diffuse and infiltrative tumors; renal failure (serum creatinine >2.0 mg/dl, or serum urea nitrogen >30 mg/dl); impaired coagulation (e.g., platelet count $<50\times10^3/\mu l$, or prothrombin activity <50%); pregnancy; or past history of choledochojejunostomy. We included those with previous treatments as well as treatment-naive cases provided that there was no local recurrence at enrollment. These inclusion criteria and the study design did not change till the study completely ended. The study design conformed to the Declaration of Helsinki Principles and was approved by the ethics committee of our institution. The study was registered at the University Hospital Medical Information Network (UMIN) Clinical Trial Registry (UMIN-CTR000000070). Written informed consent was obtained from each patient. This study complied with the CONSORT guidelines for reporting of clinical trials (27).

Study design

Before receiving RFA, patients were randomly assigned to undergo CTHA/CTAP or not in equal numbers. Patient registration and randomization were performed by computer-generated allocation at a web-based data center (Internet Data and Information Center for Medical Research) administered by UMIN. At the time of randomization, patients were stratified either as treatment naive, for whom RFA was planned as an initial treatment for HCC, or recurrent, for whom RFA was planned for recurrent HCC. The randomization was based on the Efron's biased-coin design (28). In principal, the assignment was not blinded to the investigators and the participants. The interval between random assignment and implementation of treatment for HCC was <4 weeks. CTHA/CTAP was performed on the assigned patients on the second day of admission, and RFA was performed 2 or 3 days later, given that the total number of HCC nodules remained <4. When ≥4 HCC nodules were detected on CTHA/CTAP, patients first received transarterial chemoembolization (TACE) immediately after CTHA/CTAP, followed later by RFA to achieve complete ablation of the tumor nodules.

Radiographic procedures

For the diagnosis of HCC at study entry, intravenous contrast-enhanced dynamic CT was performed on an outpatient basis using an X-ray CT device with 4, 8, or 16 detector rows (Aquilion 4/16; Toshiba, Tokyo, Japan; LightSpeed Qx/I, LightSpeed Ultra; GE Healthcare, Milwaukee, WI). Images were obtained during the early arterial, late arterial, and equilibrium phases at 28, 40, and 120 s after starting the intravenous bolus injection of iopamidol (Iopamiron; Nihon Schering, Osaka, Japan) or iohexol (Omnipaque; Daiichi Sankyo, Tokyo, Japan) at a rate of 2.3–3.3 ml/s with a power injector. The total dose of iodine was 0.7 g/kg body weight, with an upper limit of 37 g iodine. The injection time for the contrast material was 30 s. Images were reconstructed with a section thickness of 2.5 mm and a reconstruction interval of 1.5 mm, and were reviewed by experienced radiologists.

CTHA/CTAP was performed on an inpatient basis. First, a 4-Fr modified Shepherd-hook catheter and a 4-Fr hepatic-curve catheter were placed in the celiac artery and superior mesenteric artery, respectively, through bilateral femoral arteries, according to Seldinger's method. Digital subtraction angiography was performed from the celiac artery to evaluate hepatic artery anatomy. A microcatheter was inserted through the 4-Fr catheter and placed in the proper or common hepatic artery for hepatic arteriography.

The CTAP catheter was placed in the superior mesenteric artery in all cases. In the case of a replaced or accessory right hepatic artery, the catheter was inserted well beyond the origin of the hepatic artery to prevent contrast medium overflow into the hepatic artery. Less than 30 ml of contrast agent, which was diluted to 100 mg I/ml, was used before the CTHA/CTAP study. First, CTAP was performed using 90 ml nonionic contrast medium diluted to 100 mg I/ml, and then CT scanning was performed 30 s after the start of the injection at a rate of 3.0 ml/s. Multidetector-row CT images were obtained during a single breath hold in a longitudinal direction with collimation of 1 mm, table speed of 30 mm/s, 120 kVp, and

300 mAs. CTHA was performed at least 5 min after CTAP, using the same parameters. CT scanning was performed at 10 and 45 s after the start of contrast medium injection into the microcatheter at a rate of 2.0–2.5 ml/s. A total of 30–50 ml contrast agent diluted to 100 mg I/ml was used. When the liver was perfused by two or more hepatic arteries such as a replaced right hepatic artery, accessory right hepatic artery, or left hepatic artery downstream of the left gastric artery, CTHA was performed from each of the respective arteries. A diagnosis of typical HCC on CTHA/CTAP was defined as a round hypervascular nodule on CTHA with a defect on CTAP, accompanied by corona enhancement during the second phase of CTHA or hypoattenuation during the equilibrium phase of prior dynamic CT (10,29).

TACE was additionally performed when ≥4 HCC nodules were detected on CTHA/CTAP, as evaluated at the time by the operating radiologist. The procedure used 3.0 ml contrast medium, 30 mg doxorubicin (Adriacin; Kyowahakko Kirin, Tokyo, Japan), and 3.0 ml iodized oil (Lipiodol Ultra-Fluid; Guerbet Japan, Tokyo, Japan). The amounts of contrast medium and iodized oil in this suspension were arbitrarily adjusted according to tumor size. This agent was injected into each feeder of the HCC, followed by infusion of 2-mm-diameter gelatin sponge particles (Gelpart; Nihonkayaku, Tokyo, Japan).

CTHA/CTAP images were scrutinized by two experienced radiologists, who made the final diagnosis. The radiologists were not blinded to information regarding the preceding conventional dynamic CT. Preceding intravenous contrast-enhanced dynamic CT was retrospectively reviewed for nodules newly diagnosed by CTHA/CTAP to determine whether the nodules could have been detected on dynamic CT.

Radiofrequency ablation

RFA was performed on an inpatient basis. The precise procedure of RFA is described elsewhere (30). All RFA procedures were performed percutaneously under ultrasonographic guidance. We used a 17-gauge cooled-tip electrode (Cool-Tip; RF Ablation System, Covidien, Boulder, Colombia, CO) for RFA. Radiofrequency energy was delivered for 6–12 min for each application. For large tumors, the electrode was repeatedly inserted into different sites, such that the entire tumor could be enveloped by assumed necrotic volumes. A CT scan with a 5-mm section thickness was performed 1–3 days after RFA to evaluate technical effectiveness. Complete ablation was defined as hypoattenuation of the entire tumor. We intended to ablate not only the tumor but also some of the liver parenchyma surrounding it. When we suspected that some portion of tumor remained nonablated, RFA was repeated. We did not predefine the procedure number in a treatment: treatment was generally continued until CT imaging demonstrated necrosis of the entire tumor.

Follow-up

The follow-up regimen after RFA consisted of blood tests and monitoring of tumor markers in an outpatient setting. Ultrasonography and dynamic CT were performed every 4 months. Tumor recurrence was defined as a newly developed lesion on a dynamic CT that showed hyperattenuation in the arterial phase with washout in the late phase. Recurrent site was categorized as intrahepatic recurrence distant from ablated nodules, local tumor progression defined as the appearance of viable cancer tissue touching the ablated nodules, and extrahepatic metastasis (31). The follow-up was censored in February 2011 when 2 years had passed after the enrollment of patient 280. No interim analysis was specified in the protocol.

End points

The primary end point was recurrence-free survival, where both recurrence and death were treated as an event. We intended to ablate all detected nodules in both groups. When additional nodules were detected by CTHA/CTAP, the newly detected nodules were also ablated. When >3 nodules were diagnosed as HCC by CTHA/CTAP, we performed TACE and subsequently intended to ablate all of the nodules. When nonablated viable tumors were detected by CT for treatment evaluation, those cases were treated as an event 120 days after randomization. Even when newly detected nodules showed dense Lipiodol deposits after TACE, the nodules were considered as viable if the nodules were nonablated.

Secondary end points were the number of additional nodules detected by CTHA/CTAP, the proportion of patients with complete ablation, overall survival, and safety of CTHA/CTAP and RFA. Complications were defined according to the guidelines of the Society of Interventional Radiology (32). According to the guidelines, major complications were defined as those that required therapy or prolonged hospitalization, or left permanent adverse sequelae, or death.

Statistical analysis

This study was designed to detect a 15% increase in 2-year recurrence-free survival in the CTHA/CTAP group from an anticipated 35% in the control group. To detect this difference with a power of 80% and type I error of 5% (two-sided test), we needed 280 patients (140 for each arm). Differences between groups for each characteristic were tested for significance with Fisher's exact test for categorical variables and *t*-test for continuous variables. All data necessary for analysis was corrected in the main computer server system of University of Tokyo, Department of Gastroenterology.

Recurrence-free survival and overall survival were calculated using the Kaplan–Meier method and were compared by the log-rank test. Cox proportional hazard regression was used to calculate hazard ratios with 95% confidence interval (CI) between the groups in univariate and multivariate settings. The primary end point was evaluated in subgroups according to the following characteristics: age, sex, body mass index, treatment naivety, hepatitis B surface antigen (HBsAg) positivity, hepatitis C virus antibody positivity, tumor size, tumor number, platelet count, tumor marker positivity for α-fetoprotein (AFP), lens culinaris agglutinin-reactive fraction of AFP, and des-γ-carboxy prothrombin. An adjusted hazard ratio comparing the groups was calculated using multivariate Cox regression with factors that showed significance

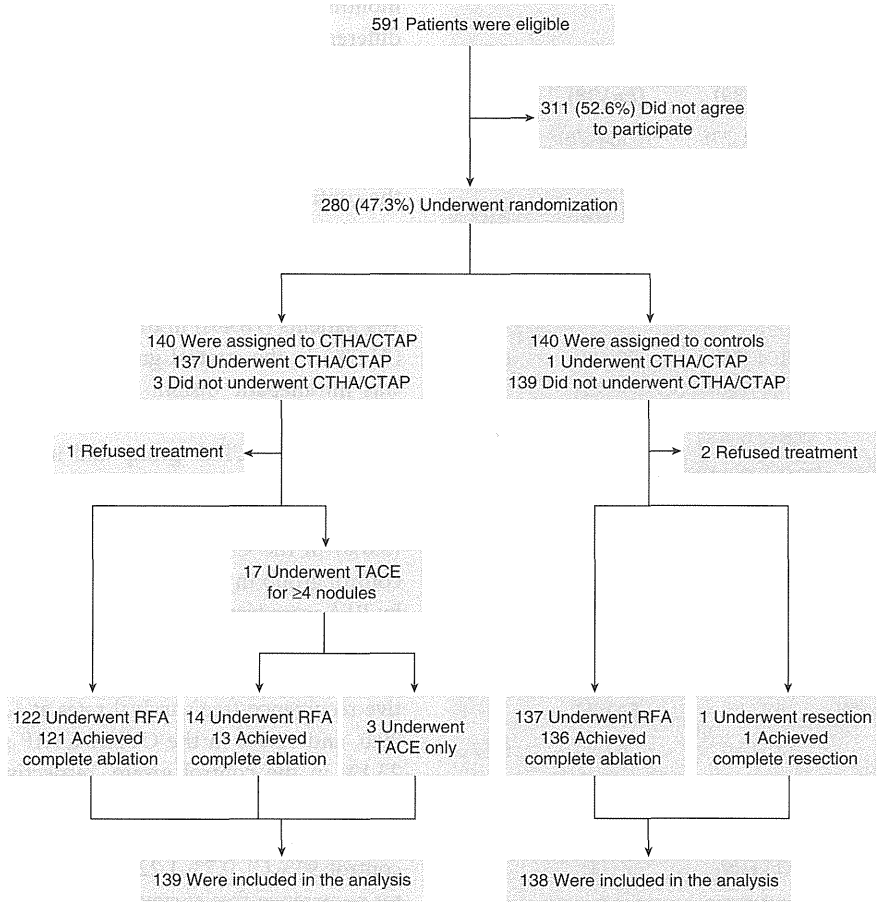

Figure 1. Patient enrollment and outcomes. CTAP, computed tomography during arterial portography; CTHA, computed tomography during hepatic arteriography; RFA, radiofrequency ablation; TACE, transarterial chemoembolization.

in univariate analysis. Data at entry were used for the analyses. A *post hoc* analysis comparing the recurrence-free survival of those with and without newly diagnosed HCC in the CTHA/CTAP group was performed.

All analyses were performed on an intention-to-treat basis. Differences with a two-sided P value of <0.05 were considered statistically significant. Data processing and analysis were performed with S-PLUS ver. 7 (TIBCO Software, Palo Alto, CA). Finally, all authors had access to the study data and had reviewed and approved the final manuscript.

RESULTS

Patient enrollment

According to the study protocol, the registration started from September 2004 for 5 years and the follow-up was censored in February 2011 when 2 years had passed after the enrollment of patient 280. During the study period, 280 of 591 (47.4%) eligible patients agreed to participate in the trial, and 140 of these were randomly assigned to undergo CTHA/CTAP before RFA. Three patients declined to undergo CTHA/CTAP after assignment. A total of 140 patients were randomly assigned to the control group. One patient assigned to the control group received CTHA/CTAP because of strong preference (**Figure 1**).

Treatment

In 45 (32.4%) patients, 75 nodules with a median diameter of 8 mm (range, 2–20) were additionally diagnosed by experienced radiologists as definite HCC on CTHA/CTAP. The detailed characteristics of newly diagnosed nodules have been reported previously (33). In 17 patients, the number of HCC nodules exceeded 3 after CTHA/CTAP, and TACE was performed subsequently. We intended to ablate all nodules by RFA including additionally detected nodules. In 122 patients, there were ≤3 HCC nodules, and complete ablation was obtained in 121 patients (99.2%). Among 17 patients treated with TACE, 14 (82.4%) subsequently underwent RFA and complete ablation was obtained in 13 (92.9%) patients. The remaining 3 patients (17.6%) did not undergo RFA because of tumor nodule multiplicity in 2 patients and simultaneously diagnosed malignant B-cell lymphoma in the third patient. Among 140 patients who were assigned to the control group, 137 (97.9%) were treated with RFA, and complete ablation was obtained in 136 (99.3%) patients. One patient withdrew consent and underwent hepatic resection. Two patients refused to receive

Table 1. Baseline characteristics of the patients[a]

Characteristics	CTHA/CTAP (*N*=139)	Control (*N*=138)	*P* value
Age, years	70 (63–74)	70 (64–75)	0.43
Male, *n* (%)	93 (67)	86 (62)	0.42
Alcohol >80 g/day, *n* (%)	23 (17)	20 (15)	0.82
BMI (kg/m^2)	23.1 (21.4–25.1)	23.4 (21.2–25.3)	0.48
Viral markers			
HCVAb positive, *n* (%)	104 (75)	99 (72)	0.59
HBsAg positive, *n* (%)	21 (15)	20 (14)	1
Serum albumin (g/dl)	3.8 (3.6–4.1)	3.9 (3.6–4.1)	0.20
Total bilirubin (mg/dl)	0.8 (0.6–1.0)	0.8 (0.6–1.0)	0.31
AST (IU/l)	56 (34–69)	57 (33–70)	0.84
ALT (IU/l)	54 (29–63)	57 (27–73)	0.61
Platelet count (×10^3/μl)	128 (89–163)	130 (91–159)	0.88
Prothrombin activity (%)	80 (72–90)	81 (74–87)	0.39
Treatment-naive case, *n* (%)	77 (55)	74 (54)	0.81
Previously treated case, n *(%)*	62 (45)	64 (46)	
Resection, *n* (%)[b]	15 (24)	16 (25)	0.27
RFA, *n* (%)[b]	46 (74)	45 (70)	
Ethanol injection, *n* (%)[b]	10 (16)	3 (4.6)	
TACE, *n* (%)[b]	11 (18)	7 (11)	
Tumor size (cm)	1.6 (1.2–2.0)	1.7 (1.2–2.0)	0.91
Single nodule, *n* (%)	101 (73)	98 (71)	0.76
AFP >100 ng/ml, *n* (%)	23 (17)	24 (17)	0.85
DCP >100 mAU/ml, *n* (%)	16 (12)	22 (16)	0.28
AFP-L3 >15%, *n* (%)	16 (12)	15 (11)	0.86

AFP, α-fetoprotein; AFP-L3, lens culinaris agglutinin-reactive fraction of AFP; ALT, alanine aminotransferase; AST, aspartate aminotransferase; BMI, body mass index; CTHA/CTAP, computed tomography during hepatic arteriography and arterial portography; DCP, des-γ-carboxy prothrombin; HBsAg, hepatitis B surface antigen; HCVAb, hepatitis C virus antibody; RFA, radiofrequency ablation, TACE, transarterial chemoembolization.

[a]Data are expressed as median (25th–75th percentiles) or number (percent).

[b]Including overlap.

any treatment and were lost to follow-up. Finally, 139 (99.3%) patients in the CTHA/CTAP group and 138 (98.6%) patients in the control group were included in the analysis.

Patient characteristics

There was no statistically significant difference in patient characteristics between the groups (**Table 1**). Median age at enrollment was 70 years, and approximately two-thirds of patients were male. Approximately 55% of patients were treatment-naive cases and the remaining patients had a history of previous treatment. Among those previously treated patients, the median interval between the initial treatment and the study enrollment was 42 (interquartile range, 22–65) months in the CTHA/CTAP group and 30 (20–61) months in the control group. There was no statistically significant difference between the two groups ($P=0.72$). The total number of HCC nodules detected in original contrast-enhanced dynamic CT was 197 (101 patients were uninodular and the rest were multinodular) in the CTHA/CTAP group and 196 (98 patients were uninodular and the rest were multinodular) in the control group.

Recurrence

By the end of the follow-up, tumor recurrence was identified in 109 patients (78.4%) in the CTHA/CTAP group and 112 patients (81.2%) in the control group. The distribution of recurrent site was intrahepatic distant recurrence ($N=98$), local tumor progression ($N=7$), both ($N=1$), and extrahepatic metastasis ($N=3$) in the CTHA/CTAP group and intrahepatic distant recurrence ($N=103$), local tumor progression ($N=4$), both ($N=2$), and extrahepatic metastasis ($N=3$) in the control group. Five patients (3.6%) in the CTHA/CTAP group and 1 patient (0.7%) in the control group in whom complete ablation could not be obtained by RFA were treated as recurrence on 120 days after randomization when the first follow-up CT would have been scheduled. In each group, four patients died without recurrence. The cumulative recurrence-free survival rates at 1, 2, and 3 years were 60.1, 29.0, and 18.9% in the CTHA/CTAP group and 52.2, 29.7, and 23.1% in the control group, respectively (**Figure 2a**). The difference between the two groups was not statistically significant ($P=0.66$ by log-rank test; hazard ratio, 0.94 for CTHA/CTAP vs. control; 95% CI, 0.73–1.22). The CTHA/CTAP group showed better recurrence-free survival with marginal statistical significance in the subgroups with higher AFP or AFP-L3 values (**Figure 3**).

Univariate Cox regression analysis identified older age ($P=0.01$), hepatitis C virus antibody positivity ($P=0.001$), lower albumin level ($P=0.04$), recurrent cases ($P<0.001$), multinodular HCC ($P<0.001$), and higher AFP level ($P=0.02$) as significant predictors for recurrence-free survival (**Table 2**). Adjusted hazard ratio of the CTHA/CTAP group vs. the control group by multivariate Cox regression analysis was 0.86 (95% CI, 0.67–1.12; $P=0.27$, **Table 3**).

Overall survival

By the end of the follow-up, 51 patients (36.7%) in the CTHA/CTAP group and 45 patients (32.6%) in the control group died. The cumulative overall survival rates at 3 and 5 years were 79.7 and 56.4% in the CTHA/CTAP group and 86.8 and 60.1% in the control group, respectively (**Figure 2b**). There was no statistically significant difference between the groups ($P=0.50$ by log-rank test; hazard ratio, 1.15, 95% CI, 0.77–1.71).

Safety

No procedural complications attributable to CTHA/CTAP or TACE were observed. Major complications related to RFA were observed in 2 patients (1.4%) in the CTHA/CTAP group (2 with neoplastic seeding) and in 3 patients (2.2%) in the control group (1 each with hepatic infarction, hemothorax, and neoplastic seeding). There was no procedure-related death.

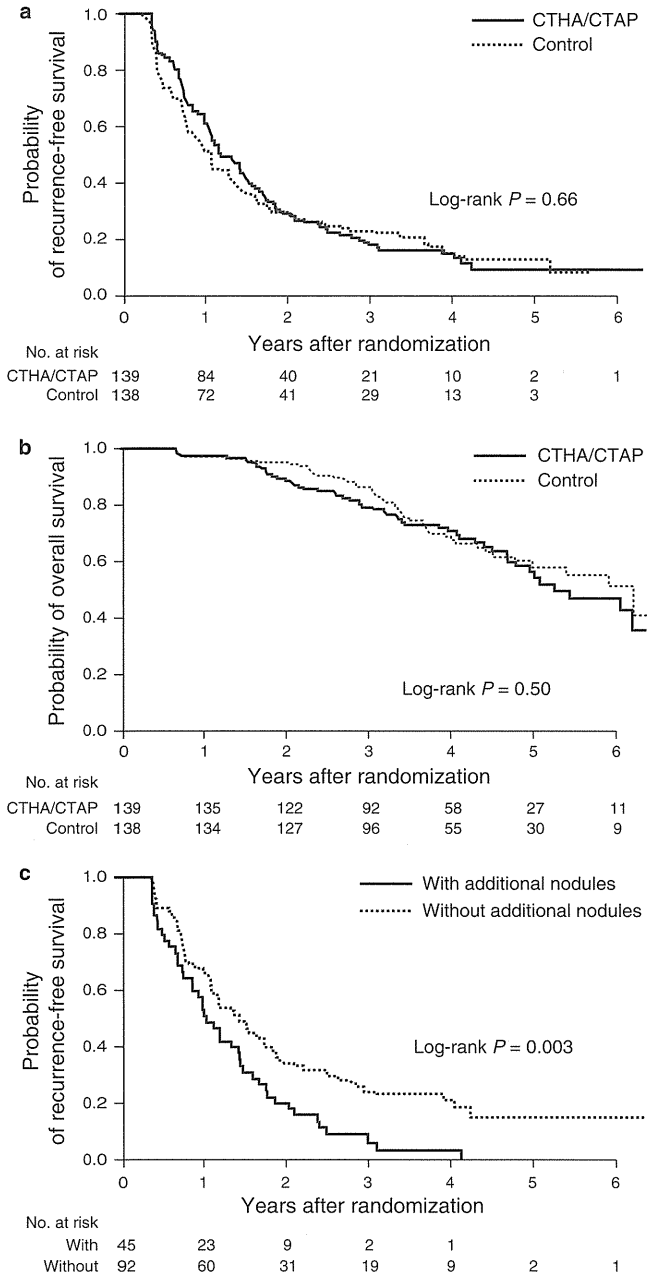

Figure 2. Kaplan–Meier estimate of the recurrence-free survival and overall survival. (**a**) The cumulative recurrence-free survival rates at 1, 2, and 3 years were 60.1, 29.0, and 18.9% in the CTHA/CTAP group and 52.2, 29.7, and 23.1% in the control group, respectively. (**b**) The cumulative overall survival rates at 3 and 5 years were 79.7 and 56.4% in CTHA/CTAP group and 86.8 and 60.1% in the control group, respectively. (**c**) Patients with an additional nodule detected by CTHA/CTAP showed significantly poorer recurrence-free survival than those without an additional nodule. CTAP, computed tomography during arterial portography; CTHA, computed tomography during hepatic arteriography.

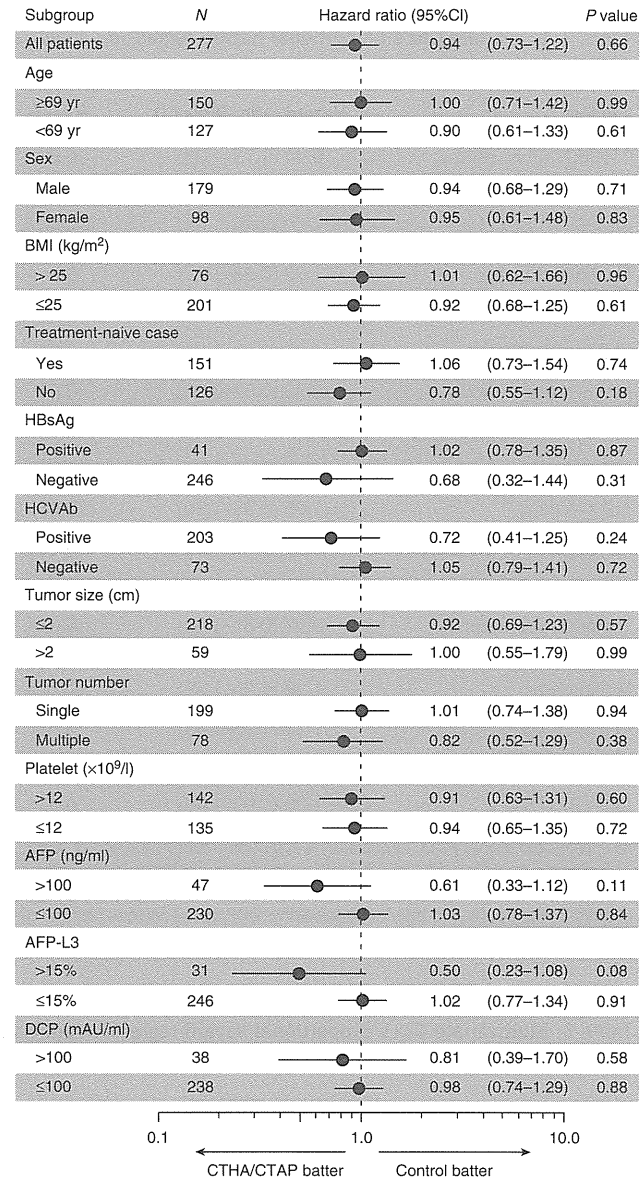

Figure 3. Recurrence-free survival of subgroups by Cox proportional hazard regression according to clinical characteristics at study entry. AFP, α-fetoprotein; BMI, body mass index; CI, confidence interval; CT, computed tomography; CTAP, computed tomography during arterial portography; CTHA, computed tomography during hepatic arteriography; DCP, des-γ-carboxy prothrombin; HBsAg, hepatitis B surface antigen; HCVAb, hepatitis C virus antibody; yr, year.

Recurrence-free survival between those with and without additional nodules in CTHA/CTAP group

As a *post hoc* analysis, we compared the recurrence-free survival between those with ($N=45$) and without ($N=92$) additional HCC nodules diagnosed by CTHA/CTAP. As compared with those in whom additional HCC nodules were not detected by CTHA/CTAP, those with additional nodules included more HBsAg-negative patients (97.7 vs. 78.3%, $P=0.002$), previously treated patients (62.2 vs. 23.9%, $P=0.006$), and patients with multiple HCC nodules on dynamic CT (44.4 vs. 17.4%, $P=0.002$). Patients with additional nodule by CTHA/CTAP showed significantly poorer

Table 2. Univariate Cox's proportional hazard regression analysis of the risk for recurrence-free survival

Variable	Hazard ratio (95% CI)	*P* value
CTHA/CTAP vs. control	0.94 (0.73–1.22)	0.66
Age (per year)	1.02 (1.00–1.04)	0.01
Female vs. male	1.02 (0.78–1.34)	0.88
Alcohol >80 g/day	1.02 (0.88–1.17)	0.81
HCVAb positive	1.69 (1.23–2.31)	0.001
BMI (per 1.0 kg/m^2)	1.02 (0.98–1.06)	0.35
Albumin (per 1.0 g/dl)	0.72 (0.52–0.98)	0.04
Total bilirubin (per 1.0 mg/dl)	1.02 (0.97–1.07)	0.51
AST >40 IU/l	1.14 (0.99–1.31)	0.07
ALT >40 IU/l	1.05 (0.92–1.20)	0.45
Platelet count >10×10^3/μl	0.89 (0.78–1.01)	0.08
Recurrent case	2.33 (1.79–3.02)	<0.001
Tumor size of maximal nodule >2.0 cm	0.97 (0.85–1.10)	0.62
Multinodular	1.38 (1.20–1.59)	<0.001
AFP >100 ng/ml	1.21 (1.03–1.43)	0.02
DCP >100 mAU/ml	0.99 (0.82–1.20)	0.93
AFP-L3 >15%	1.20 (0.99–1.46)	0.07

AFP, α-fetoprotein; AFP-L3, lens culinaris agglutinin-reactive fraction of AFP; ALT, alanine aminotransferase; AST, aspartate aminotransferase; BMI, body mass index; CI, confidence interval; CTHA/CTAP, computed tomography during hepatic arteriography and arterial portography; DCP, des-γ-carboxy prothrombin; HCVAb, hepatitis C virus antibody.

Table 3. Multivariate Cox's proportional hazard regression analysis of the risk for recurrence-free survival

Variable	Hazard ratio (95% CI)	*P* value
CTHA/CTAP vs. control	0.86 (0.0.67–1.12)	0.27
Age (per year).	1.01 (0.99–1.02)	0.36
HCVAb positive	1.36 (0.98–1.89)	0.07
Albumin (per 1.0 g/dl)	0.75 (0.53–1.07)	0.11
Recurrent case	2.21 (1.69–2.89)	<0.001
Multinodular	1.69 (1.27–2.25)	<0.001
AFP >100 ng/ml	1.41 (0.996–1.98)	0.052

AFP, α-fetoprotein; CI, confidence interval; CTHA/CTAP, computed tomography during hepatic arteriography and arterial portography; HCVAb, hepatitis C virus antibody.

recurrence-free survival than those without additional nodules ($P=0.003$, **Figure 2c**).

DISCUSSION

An advance in diagnostic technology generally indicates improved sensitivity or specificity, which corresponds to the detection of smaller lesions with a clearer view in imaging modalities. In our previous study, we showed that 75 nodules with a mean diameter of 8.7 mm (range, 2–20 mm) in 45 (33%) of 139 patients who underwent CTHA/CTAP were additionally diagnosed as definite HCC, compared with dynamic CT examination (33). However, no significant difference was observed in terms of recurrence-free survival between those who did and did not undergo CTHA/CTAP before RFA.

One reason for this discrepancy may be that the impact of CTHA/CTAP on recurrence reduction was diluted by a long-term follow-up of >2 years. It is unlikely that CTHA/CTAP could detect small nodules that would be detected ≥2 years later by conventional dynamic CT. In fact, the number of recurrences identified within 1 year after enrollment was lower in the CTHA/CTAP group than the control group (54 vs. 65, data not shown).

Another reason could be that fewer patients achieved complete ablation of target nodules in the CTHA/CTAP group than in the control group. The additionally diagnosed HCC nodules were small, and detection of these nodules by ultrasonography was difficult. Recent technologies such as contrast ultrasonography or fusion imaging, which can improve the accuracy of ablation techniques (34–36), may increase the probability of detection of smaller nodules before RFA.

Precise evaluation of the stage of progression is important for deciding on treatment procedures in HCC management. Seventeen patients in the CTHA/CTAP group were diagnosed with ≥4 nodules by CTHA/CTAP, which is not considered suitable for RFA according to widely used criteria.

In our previous study, we showed that recurrence as opposed to initial occurrence, multinodularity on dynamic CT, and HBsAg negativity were significant predictors for finding additional HCC by CTHA/CTAP (33). In fact, the CTHA/CTAP group showed better outcomes in the subgroups with HBsAg-negative cases, previously treated patients, and multinodular HCC. However, *post hoc* analysis comparing recurrence-free survival of those with and without additional nodules detected by CTHA/CTAP showed that those with a higher probability of additional nodules were also at a higher risk of recurrence. The advantage of CTHA/CTAP in finding more HCC nodules might be counter balanced by the higher risk of recurrence.

This study has several limitations. First, the additional nodules detected by CTHA/CTAP were not confirmed histologically. Therefore, we cannot exclude the possibility of overdiagnosis. Second, 45% of the patients had a history of previous treatment including resection, RFA, and TACE. Those previous treatments might substantially alter the hemodynamic status in the liver and affect the accuracy of CTHA/CTAP. On the other hand, in the previously treated cases, the radiologists could refer to the past series of dynamic CT during performing CTHA/CTAP, which might improve the accuracy of CTHA/CTAP as compared with treatment-naive cases. Third, 17 patients in the CTHA/CTAP group underwent TACE as a salvage treatment because total number of HCC nodules exceeded 3 after CTHA/CTAP. This might affect the recurrence-free and overall survival in the CTHA/CTAP group.

Our results may be extrapolated to other imaging modalities including gadoxetic acid–enhanced magnetic resonance imaging and second-generation contrast ultrasonography (37,38). These newly developed modalities also make possible the detection of small nodules that are invisible by dynamic CT. However, better diagnosis does not necessarily lead to better primary outcome.

In conclusion, CTHA/CTAP before RFA resulted in improved HCC diagnosis and detection of additional nodules in one-third of the study participants. However, it did not improve recurrence-free survival. The indications for CTHA/CTAP should be evaluated carefully.

Study protocol URL: https://upload.umin.ac.jp/cgi-open-bin/ctr/ctr.cgi?function=brows&action=brows&recptno=R000000117&type=summary&language=E.

CONFLICT OF INTEREST

Guarantor of the article: Ryosuke Tateishi, MD, PhD.

Specific author contributions: Conception and design: R.T., M.A., N.Y., T.G., S.S., H.Y., Y.M., and M.O.; analysis: R.T. and Y.M.; treatment and data collection: T.O., R.T., M.A., S.M., M.S., K.U., T.A., K.E., Y.K., T.G., and S.S.; drafting article: T.O.; critical revision: R.T., M.A., H.Y., K.O., and K.K.

Financial support: This work was supported by Health Sciences Research grants of The Ministry of Health, Labour and Welfare of Japan (Research on Hepatitis). No additional external funding was received for this study. The funders had no role in study design, data collection and analysis, decision to publish, or preparation of the manuscript.

Potential competing interests: None.

Study Highlights

WHAT IS CURRENT KNOWLEDGE

- ✓ Computed tomography with hepatic arteriography and arterial portography (CTHA/CTAP) give higher hepatocellular carcinoma (HCC) detection sensitivity than conventional dynamic enhanced CT.
- ✓ CTHA/CTAP is an invasive procedure requiring the insertion of an intraarterial catheter through a femoral puncture.
- ✓ The indication for CTHA/CTAP can be justified only when the expected benefits exceed the risks and cost of the procedure.

WHAT IS NEW HERE

- ✓ Our study is the first randomized controlled trial (RCT) to evaluate the utility of CTHA/CTAP before radiofrequency ablation (RFA) in patients with HCC in the whole world.
- ✓ The best candidates for CTHA/CTAP were patients with multinodular HCC, and recurrent cases after previous treatment.
- ✓ However, CTHA/CTAP before RFA did not improve cumulative recurrence-free survival or overall survival.
- ✓ These observations are clinically important as the technique had limited utility and highlights the observation that patient outcomes are probably not related to the presence of small liver nodules.
- ✓ These findings reinforce the notion of genetic determinants of HCC recurrence.

REFERENCES

1. El-Serag HB, Mason AC. Rising incidence of hepatocellular carcinoma in the United States. N Engl J Med 1999;340:745–50.
2. Kiyosawa K, Umemura T, Ichijo T *et al.* Hepatocellular carcinoma: recent trends in Japan. Gastroenterology 2004;127:S17–26.
3. Itai Y, Matsui O. Blood flow and liver imaging. Radiology 1997;202:306–14.
4. Matsui O. Detection and characterization of hepatocellular carcinoma by imaging. Clin Gastroenterol Hepatol 2005;3:S136–40.
5. Teratani T, Yoshida H, Shiina S *et al.* A novel display of reconstruction computed tomography for the detection of small hepatocellular carcinoma. Liver Int 2004;24:619–24.
6. Fujishima T, Yoshida H, Obi S *et al.* Analysis of factors influencing hepatocellular carcinoma detection: efficient use of computed tomography during arterial portography and during hepatic arteriography. J Gastroenterol 2005;40:266–73.
7. Sangiovanni A, Manini MA, Iavarone M *et al.* The diagnostic and economic impact of contrast imaging techniques in the diagnosis of small hepatocellular carcinoma in cirrhosis. Gut 2010;59:638–44.
8. Murakami T, Oi H, Hori M *et al.* Helical CT during arterial portography and hepatic arteriography for detecting hypervascular hepatocellular carcinoma. AJR Am J Roentgenol 1997;169:131–5.
9. Kanematsu M, Hoshi H, Imaeda T *et al.* Detection and characterization of hepatic tumors: value of combined helical CT hepatic arteriography and CT during arterial portography. AJR Am J Roentgenol 1997;168:1193–8.
10. Irie T, Takeshita K, Wada Y *et al.* CT evaluation of hepatic tumors: comparison of CT with arterial portography, CT with infusion hepatic arteriography, and simultaneous use of both techniques. AJR Am J Roentgenol 1995;164:1407–12.
11. Small WC, Mehard WB, Langmo LS *et al.* Preoperative determination of the resectability of hepatic tumors: efficacy of CT during arterial portography. AJR Am J Roentgenol 1993;161:319–22.
12. Soyer P, Levesque M, Elias D *et al.* Detection of liver metastases from colorectal cancer: comparison of intraoperative US and CT during arterial portography. Radiology 1992;183:541–4.
13. Soyer P, Levesque M, Elias D *et al.* Preoperative assessment of resectability of hepatic metastases from colonic carcinoma: CT portography vs sonography and dynamic CT. AJR Am J Roentgenol 1992;159:741–4.
14. Matsui O, Kadoya M, Suzuki M *et al.* Work in progress: dynamic sequential computed tomography during arterial portography in the detection of hepatic neoplasms. Radiology 1983;146:721–7.
15. Sherman M, Klein A. AASLD single-topic research conference on hepatocellular carcinoma: conference proceedings. Hepatology 2004;40:1465–73.
16. Tateishi R, Shiina S, Ohki T *et al.* Treatment strategy for hepatocellular carcinoma: expanding the indications for radiofrequency ablation. J Gastroenterol 2009;44 (Suppl 19): 142–6.
17. Ebara M, Ohto M, Sugiura N *et al.* Percutaneous ethanol injection for the treatment of small hepatocellular carcinoma. Study of 95 patients. J Gastroenterol Hepatol 1990;5:616–26.
18. Livraghi T, Giorgio A, Marin G *et al.* Hepatocellular carcinoma and cirrhosis in 746 patients: long-term results of percutaneous ethanol injection. Radiology 1995;197:101–8.
19. Shiina S, Tagawa K, Niwa Y *et al.* Percutaneous ethanol injection therapy for hepatocellular carcinoma: results in 146 patients. AJR Am J Roentgenol 1993;160:1023–8.
20. Seki T, Wakabayashi M, Nakagawa T *et al.* Percutaneous microwave coagulation therapy for patients with small hepatocellular carcinoma: comparison with percutaneous ethanol injection therapy. Cancer 1999;85:1694–702.
21. Rossi S, Di Stasi M, Buscarini E *et al.* Percutaneous RF interstitial thermal ablation in the treatment of hepatic cancer. AJR Am J Roentgenol 1996;167:759–68.
22. Allgaier HP, Deibert P, Zuber I *et al.* Percutaneous radiofrequency interstitial thermal ablation of small hepatocellular carcinoma. Lancet 1999;353:1676–7.
23. Livraghi T, Goldberg SN, Lazzaroni S *et al.* Small hepatocellular carcinoma: treatment with radio-frequency ablation versus ethanol injection. Radiology 1999;210:655–61.
24. Curley SA, Izzo F, Ellis LM *et al.* Radiofrequency ablation of hepatocellular cancer in 110 patients with cirrhosis. Ann Surg 2000;232:381–91.
25. Shiina S, Tateishi R, Arano T *et al.* Radiofrequency ablation for hepatocellular carcinoma: 10-year outcome and prognostic factors. Am J Gastroenterol 2012;107:569–77; quiz 578.
26. Jang HJ, Lim JH, Lee SJ *et al.* Hepatocellular carcinoma: are combined CT during arterial portography and CT hepatic arteriography in addition to

triple-phase helical CT all necessary for preoperative evaluation? Radiology 2000;215:373–80.
27. Rennie D. CONSORT revised--improving the reporting of randomized trials. JAMA 2001;285:2006–7.
28. Efron B. Forcing a sequential experiment to be balanced. Biometrika 1971;58:403.
29. Kitao A, Zen Y, Matsui O *et al.* Hepatocarcinogenesis: multistep changes of drainage vessels at CT during arterial portography and hepatic arteriography--radiologic-pathologic correlation. Radiology 2009;252:605–14.
30. Tateishi R, Shiina S, Teratani T *et al.* Percutaneous radiofrequency ablation for hepatocellular carcinoma. An analysis of 1000 cases. Cancer 2005;103:1201–9.
31. Goldberg SN, Grassi CJ, Cardella JF *et al.* Image-guided tumor ablation: standardization of terminology and reporting criteria. J Vasc Interv Radiol 2009;20:S377–90.
32. Sacks D, McClenny TE, Cardella JF *et al.* Society of Interventional Radiology clinical practice guidelines. J Vasc Interv Radiol 2003;14:S199–202.
33. Ohki T, Tateishi R, Akahane M *et al.* Characteristics of hepatocellular carcinoma nodules newly detected by computed tomography during arteriography and arterial portography: preliminary report of a randomized controlled trial. Hepatol Int 2011 (e-pub ahead of print).
34. Minami Y, Kudo M. Review of dynamic contrast-enhanced ultrasound guidance in ablation therapy for hepatocellular carcinoma. World J Gastroenterol 2011;17:4952–9.
35. Numata K, Fukuda H, Morimoto M *et al.* Use of fusion imaging combining contrast-enhanced ultrasonography with a perflubutane-based contrast agent and contrast-enhanced computed tomography for the evaluation of percutaneous radiofrequency ablation of hypervascular hepatocellular carcinoma. Eur J Radiol 2012;81:2746–53.
36. Masuzaki R, Shiina S, Tateishi R *et al.* Utility of contrast-enhanced ultrasonography with Sonazoid in radiofrequency ablation for hepatocellular carcinoma. J Gastroenterol Hepatol 2011;26:759–64.
37. Ichikawa T, Saito K, Yoshioka N *et al.* Detection and characterization of focal liver lesions: a Japanese phase III, multicenter comparison between gadoxetic acid disodium-enhanced magnetic resonance imaging and contrast-enhanced computed tomography predominantly in patients with hepatocellular carcinoma and chronic liver disease. Invest Radiol 2010;45:133–41.
38. Hatanaka K, Kudo M, Minami Y *et al.* Differential diagnosis of hepatic tumors: value of contrast-enhanced harmonic sonography using the newly developed contrast agent, Sonazoid. Intervirology 2008; 51 (Suppl 1): 61–9.

SCIENTIFIC REPORTS

OPEN

SUBJECT AREAS:
TUMOUR IMMUNOLOGY
CANCER PREVENTION
LIVER CANCER
TRANSLATIONAL RESEARCH

Received
2 May 2013

Accepted
4 September 2013

Published
24 September 2013

Correspondence and requests for materials should be addressed to M.O. (otsukamo-tky@umin.ac.jp)

* These authors contributed equally to this work.

Regulation of the expression of the liver cancer susceptibility gene MICA by microRNAs

Takahiro Kishikawa[1]*, Motoyuki Otsuka[1,2]*, Takeshi Yoshikawa[1], Motoko Ohno[1], Akemi Takata[1], Chikako Shibata[1], Yuji Kondo[1], Masao Akanuma[3], Haruhiko Yoshida[1] & Kazuhiko Koike[1]

[1]Department of Gastroenterology, Graduate School of Medicine, The University of Tokyo, Tokyo 113-8655, Japan, [2]Japan Science and Technology Agency, PRESTO, Kawaguchi, Saitama 332-0012, Japan, [3]Division of Gastroenterology, The Institute for Adult Diseases, Asahi Life Foundation, Tokyo 100-0005, Japan.

Hepatocellular carcinoma (HCC) is a threat to public health worldwide. We previously identified the association of a single nucleotide polymorphism (SNP) at the promoter region of the MHC class I polypeptide-related sequence A (MICA) gene with the risk of hepatitis-virus-related HCC. Because this SNP affects MICA expression levels, regulating MICA expression levels may be important in the prevention of HCC. We herein show that the microRNA (miR) 25-93-106b cluster can modulate MICA levels in HCC cells. Overexpression of the miR 25-93-106b cluster significantly suppressed MICA expression. Conversely, silencing of this miR cluster enhanced MICA expression in cells that express substantial amounts of MICA. The changes in MICA expression levels by the miR25-93-106b cluster were biologically significant in an NKG2D-binding assay and an *in vivo* cell-killing model. These data suggest that the modulation of MICA expression levels by miRNAs may be a useful method to regulate HCCs during hepatitis viral infection.

Hepatocellular carcinoma (HCC) is the third most common cause of cancer-related mortality worldwide[1]. Although multiple major risk factors have been identified, such as genetic factors, environmental toxins, alcohol abuse, obesity, and metabolic disorders[2], infection with hepatitis virus B (HBV) or C (HCV) remains the major etiological factor for HCC[1].

Disease progression in HBV-induced or HCV-induced HCC is a multistep phenomenon. The clinical outcomes vary among individuals[1,3,4] because disease progression is influenced by both environmental and genetic risk factors. In terms of genetic susceptibility factors for HCV-induced HCC, we previously identified a single nucleotide polymorphism (SNP) site in the 5′-flanking region of the MICA gene on 6p21.33 (rs2596452) that is strongly associated with progression from chronic hepatitis C to HCC[5]. Individuals with the risk allele A of rs2596452 showed lower serum MICA protein levels[5]. Our subsequent study revealed that the same SNP site was also significantly associated with the risk of HBV-induced HCC[6]. However, interestingly, the risk allele was G in cases of HBV infection, which differed from HCV infection, and the individuals with the risk allele showed increased MICA protein expression levels[6]. Despite the different risk alleles at the same SNP site and inverse association between serum MICA levels and HCC risks in these two etiologies, MICA protein expression levels are significantly associated with susceptibility to HCC in chronic hepatitis viral infection.

MICA is highly expressed on viral-infected and cancer cells and acts as a ligand for NKG2D to activate the antitumor effects of natural killer cells and CD8 T cells[7,8]. This NKG2D-mediated tumor rejection is considered to be effective in the early stages of tumor growth[9–11]. Thus, the expression levels of MICA on the tumor cell surface may determine the antitumor efficacy, and the levels of shedding MICA in serum may act as a decoy of NKG2D to avoid tumor rejection.

Although several stress pathways regulate the transcription of the MICA gene[12,13], cellular microRNAs are suggested to control MICA protein expression via post-transcriptional mechanisms[14,15]. Recently, nucleic-acid-mediated gene therapy has been undergoing clinical trials[16]. Therefore, to target the clinical application of our GWAS results toward prevention of chronic-hepatitis-infection-induced HCC by nucleic-acid-mediated therapy, we determined the regulatory mechanisms of MICA protein expression using miRNA overexpression and miRNA functional silencing.

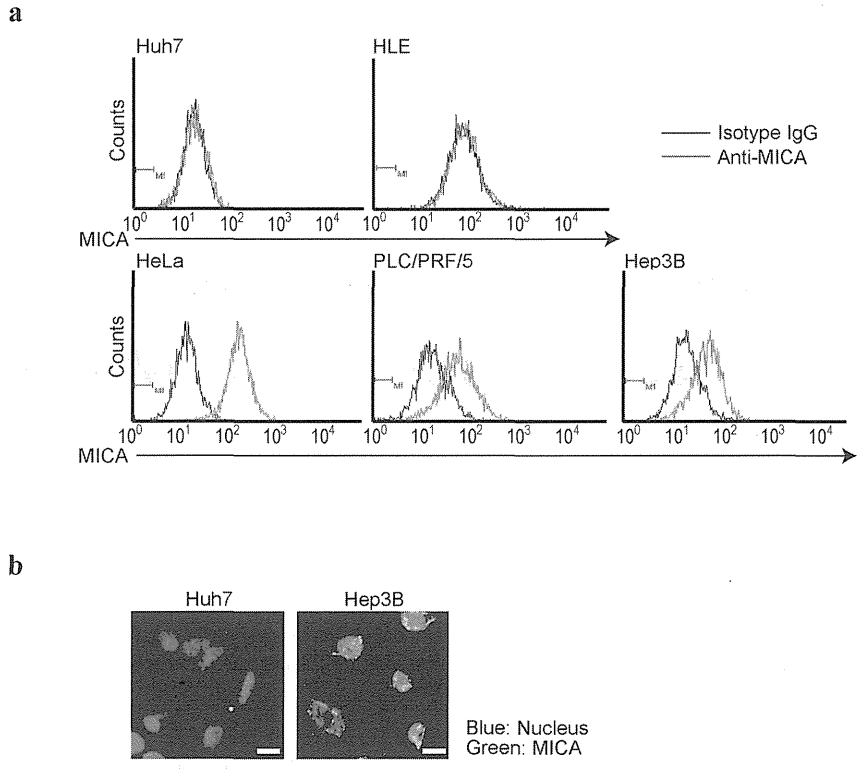

Figure 1 | Expression of MICA protein in HCC cells. (a), Flow cytometry assessment of MICA protein expression in HCC cells (purple lines). Isotype IgG was used for background staining (black lines). HeLa cells were used as the positive control. Representative results from two independent experiments are shown. (b), Immunofluorescence staining for MICA in Huh7 and Hep3B cells. Representative images from two independent experiments are shown. Scale bar, 25 μm.

Results

HCC cell lines differentially express MICA protein. To determine MICA protein levels in HCC cells, four representative HCC cell lines (Huh7, HLE, PLC/PRF/5, and Hep3B cells) underwent flow cytometry to evaluate MICA protein expression because no appropriate antibodies against MICA protein are at present available for western blotting. HeLa cells, which are known to express MICA protein[17], were used as a positive control. Hep3B and PLC/PRF/5 cells expressed substantial MICA protein levels, Huh7 and HLE cells expressed no MICA protein (Figure 1a). This was confirmed by immunocytochemistry using Huh7 and Hep3B cells, which showed staining mainly of cell surfaces (Figure 1b). These results suggest that the MICA protein expression status depends on the cell line examined, even those from the same organ.

The MiR25-93-106b cluster regulates MICA expression. Because upregulation of MICA expression was observed in Dicer-knockdown cells[18], we hypothesized that MICA expression levels may be at least partly regulated by miRNAs. We initially tested miRNAs that might affect MICA expression using reporter constructs into which MICA 3′-untranslated region (3′UTR) sequences were cloned and by transiently overexpressing 76 mature synthetic microRNAs, which were selected on the basis of their hepatic expression level, as in our previous studies[19,20]. Among the microRNAs examined, several may target MICA 3′UTR (Supplementary Figure 1). Among them, we focused on miR93 and miR106b, which were considered to target MICA 3′UTR based partly on the results of our initial miRNA testing described above; in addition, their possible target sequences were identified in the MICA 3′UTR sequences by a computational search using TargetScan 6.0 [21]. Additional reasons that we focused on these two miRNAs were as follows: 1) these miRNAs share the same seed sequences, to which two perfect-match complementary sequences exist in the 3′UTR of MICA (Figure 2a); 2) the target sequences are highly conserved among mammals and are thus likely to be biologically important sites; and 3) these miRNAs are located as a "miR25-93-106b cluster" on human chromosome 7q22.1, and so they may be expressed together under the same transcriptional control. We introduced mutations in the first possible miRNA target sequences of MICA 3′UTR in the reporter constructs (Supplementary Figure 2a); these sequences have a higher likelihood to be target sites, as determined by TargetScan. Co-transfection experiments revealed that reporter activity was suppressed by overexpression of a miR25-93-106b cluster-expressing plasmid (Figure 2b and Supplementary Figure 2b). The overexpression of an unrelated miR (let-7g)-expressing plasmid did not have any significant effects on the reporter activity (Supplementary Figure 2c) and the suppressive effect was lost using constructs with three point mutations in the seed sequences (Figure 2c), suggesting that miR25-93-106b directly targets these sequences and suppresses gene expression.

To confirm these effects, we generated HeLa and Hep3B cell lines that stably expressed the miR25-93-106b-cluster by transducing cells with miR25-93-106b-cluster-expressing lentiviruses (Figure 2d). As expected, the expression of the miR25-93-106b-cluster significantly suppressed MICA protein expression (Figure 2e). However, the expression levels of endogenous miR93 and 106b were not always proportional to the levels of MICA protein expression in the cell lines examined (Supplementary Figure 3). These results suggest that MICA protein expression can be regulated by miR93 and 106b, but that its expression is simultaneously endogenously regulated by other factors (possibly by promoter activities, including epigenetic changes).

Inhibition of miR25-93-106b function increases MICA protein expression. To develop methods of enhancing MICA protein expression levels based on the above results, we examined the

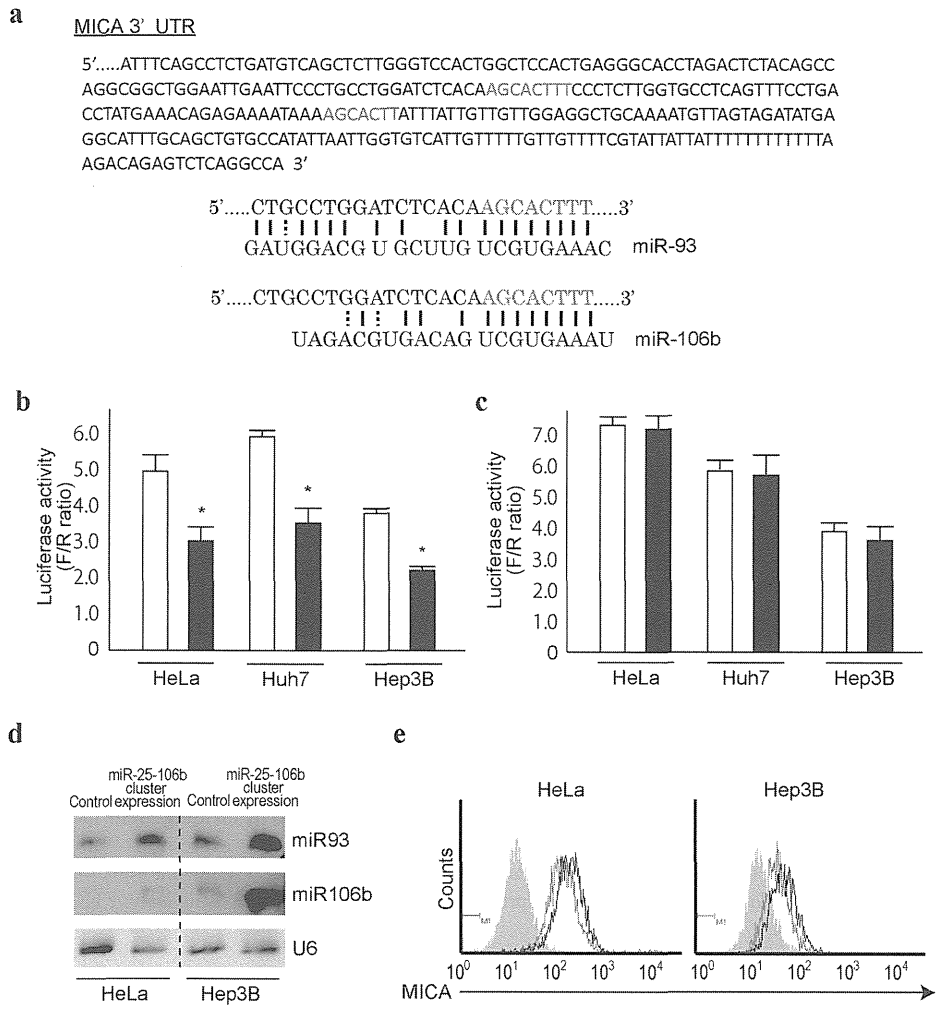

Figure 2 | miR93 and 106b target MICA 3′UTR. (a), Sequences of MICA 3′UTR (upper). Letters in red are the sequences completely matched with the seed regions of miR93 and 106b. The complementarities between the first predicted target in the MICA 3′UTR and miRNA sequences are shown below. (b), (c), Cells were co-transfected with pGL4-TK (renilla luciferase as an internal control), Luc-MICA-3′UTRwt (b) or Luc-MICA-3′UTRmut (c), and either an empty control vector (white bar) or miR25-93-106b-cluster expression plasmid (black bar). Data shows the means ± s.d. of the raw ratios (F/R) obtained by dividing firefly luciferase values with renilla luciferase values of three independent experiments. $*p < 0.05$. (d), miR93 and miR106b expression levels in control and stably miR25-93-106b cluster-expressing cells were determined by northern blotting. U6 levels were used as a loading control. Representative images from two independent experiments are shown. Full-length blot images are available in Supplementary Figure 5. (e), Suppression of MICA expression by overexpression of miRNA93 and 106b. Flow cytometry assessment of MICA protein expression in control (black lines) and stably miR25-93-106b cluster-expressing HeLa and Hep3B cells (red lines). Gray-shaded histograms represent the background staining using isotype IgG. Representative results from two independent experiments are shown.

effects of functional downregulation of miR25-93-106b on MICA expression. We first performed a reporter assay of transient functional silencing of miR25-93-106b using a construct that produces mature anti-sense RNAs designed to silence miR25-93-106b function. As expected, the reporter activities with MICA 3′UTR sequences were enhanced by the functional silencing of miR25-93-106b in HeLa, Hep3B, and Huh7 cells (Figure 3a). However, such effects were not observed using mutant reporter constructs not targeted by those miRNAs (Figure 3b), suggesting that the enhancing effects of the reporter activities were miRNA-dependent.

Next, HeLa, Hep3B, and Huh7 cells were stably transduced with a lentivirus that expresses anti-sense RNAs as described above, and MICA protein expression levels were determined by flow cytometry. Consistent with the reporter assay results, MICA protein expression was increased in HeLa and Hep3B cells by the functional silencing of miR25-93-106b (Figure 3c). However, in Huh7 cells, which express no MICA protein in the normal state, silencing of miR25-93-106b had no effect on MICA protein expression (Figure 3c). These results suggest that MICA protein expression levels can be regulated by modulating miRNA function, albeit only if at least a small quantity of MICA protein is present. In contrast, modulation of miRNA function does not influence MICA protein expression levels when the MICA protein is not expressed, but this could be because there are other forms of regulation at extremely low levels.

MICA protein levels are related to tumor susceptibility to NK cells. To determine the consequences of the modulation of MICA protein expression levels by miRNAs, we first determined the binding ability of NKG2D, a receptor of MICA, using HeLa and Hep3B cells overexpressing the miR25-93-106b cluster or with silencing of miR25-93-106b function. As expected, the levels of NKG2D binding to the cells, theoretically through binding to MICA, were decreased in HeLa and Hep3B cells overexpressing the miR25-93-106b cluster (Figure 4a). On the contrary, the levels of NKG2D binding to the cells were increased in HeLa and Hep3B cells in which miR25-93-106b function had been silenced (Figure 4b).

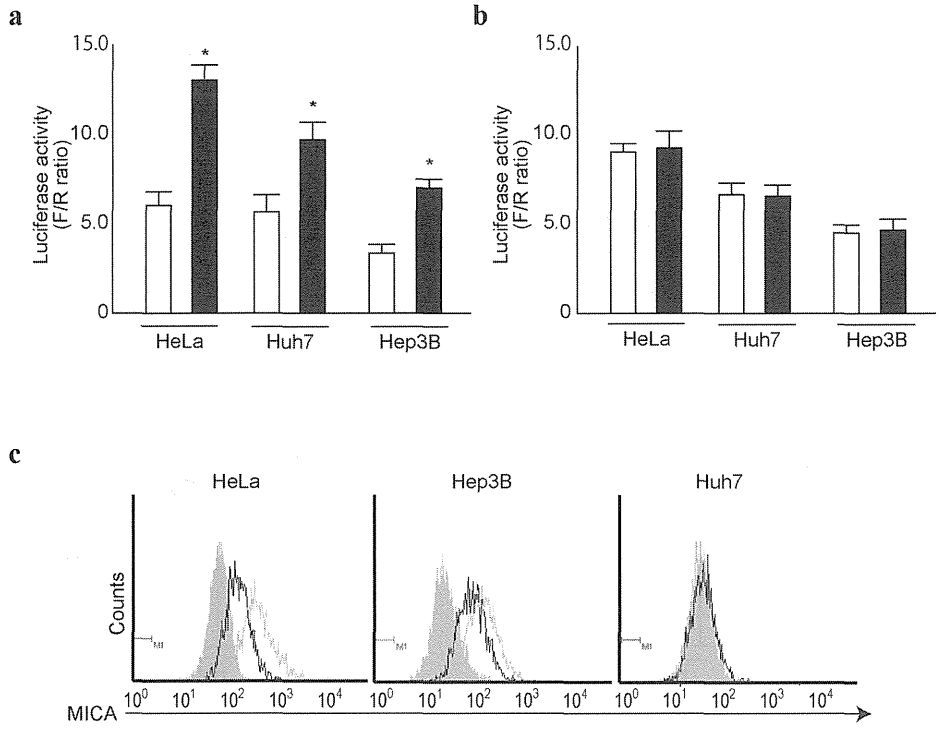

Figure 3 | Silencing of miR25-93-106b cluster enhances MICA expression. (a), (b), Cells were co-transfected with pGL4-TK (internal control), Luc-MICA-3′UTRwt (a) or Luc-MICA-3′UTRmut (b), and either an empty control vector (white bar) or plasmid expressing mature anti-sense sequences of miR25-93-106b cluster (black bar). Data shows the means ± s.d. of the raw ratios (F/R) obtained by dividing firefly luciferase values with renilla luciferase values of three independent experiments. $*p < 0.05$. (c), Enhancement of MICA expression by expression of anti-sense sequences of the miR25-93-106b cluster. Flow cytometry assessment of MICA protein expression in control (black lines) and stably mature anti-sense sequences of miR25-93-106b cluster-expressing cells (green lines). Gray-shaded histograms represent the background staining using isotype IgG. Representative results from three independent experiments are shown.

Next, to determine whether tumor cells with different miRNA-induced MICA protein expression levels exhibited differing susceptibilities to NK-cell-mediated killing *in vivo*, we performed a tumor-clearance assay that measures short-term *in vivo* killing by NK cells[22]. Hep3B control cells, Hep3B cells with miR25-93-106b cluster overexpression, or Hep3B cells with miR25-93-106b and HA-tagged MICA overexpression, labeled with fluorescent DiO, were injected into C57Black6/J mouse tail veins together with an equal number of HeLa cells labeled with Dil (internal reference control). After 5 h, surviving Hep3B and HeLa cells in the lungs were enumerated by flow cytometry. The number of Hep3B cells that had survived divided by the number of HeLa cells that had survived represents the relative killing of Hep3B cells *in vivo*. As shown by the *in vitro* binding assay using NKG2D, the killing rate of Hep3B cells in which miRNA function had been silenced was higher, and that of cells overexpressing miRNAs was lower, than that of control cells. The effects of miRNA overexpression were similar to those obtained in MICA knocked-down Hep3B cells (supplementary Figure 4). Additionally, the lower cell-killing rate in Hep3B cells overexpressing miRNA was antagonized by the co-expression of exogenous MICA protein (Figure 4c), suggesting that the decreased clearance was mediated by reduced MICA expression levels secondary to overexpression of miRNAs. These results suggest that tumor progression and invasion can be regulated by expression or silencing of miRNAs in at least some cells by regulation of MICA expression levels.

Discussion

In this study, we showed that the miR25-93-106b cluster modulates MICA protein expression by HCC cells. Because our previous GWAS analyses identified that MICA is the critical gene determining HCC susceptibility in patients with chronic hepatitis infection[5,6], the herein-described methods of modulating MICA expression may be useful for developing novel methods of prevention and therapeutics against HCCs.

MICA is a membrane protein that acts as a ligand for NKG2D to activate innate anti-tumor effects through natural killer and $CD8^+$ cells[7]. Our previous GWAS study showed that a risk allele at the SNP in the MICA promoter region was significantly associated with the susceptibility of HCV-induced HCC as well as with lower serum MICA levels. Although polymorphisms at the same SNP site were also associated with HBV-induced HCC, the risk allele determining the susceptibility of HCC was somehow different from that in HCV-induced HCC. While the reason why different MICA gene variations act as risk alleles at the same SNP site between HBV- and HCV-induced HCC has not been elucidated, it is assumed that changes in the membrane-bound MICA and soluble MICA levels due to differences in post-translational processing according to virus type may affect the risk allele results. In any case, because the importance of the regulation of MICA expression levels to prevent development of HCC due to chronic hepatitis viral infection cannot be denied, the regulation of MICA levels by microRNAs as shown here may be useful for the development of preventive methods of preventing HCC development during chronic hepatitis infection.

While several cellular signaling pathways lead to upregulation of MICA[12,13], we used microRNAs to regulate the expression levels of MICA in this study. As shown by the results of our GWAS analyses, which found that the polymorphisms in the promoter region of MICA are associated with changes in the sMICA levels[5,6], promoter activities of the MICA gene also have significant effects on MICA expression levels[23]. Our results showed that miR93 and 106b expression levels were not always correlated with those of MICA in HCC cell lines, suggesting that the regulation of MICA expression is not solely

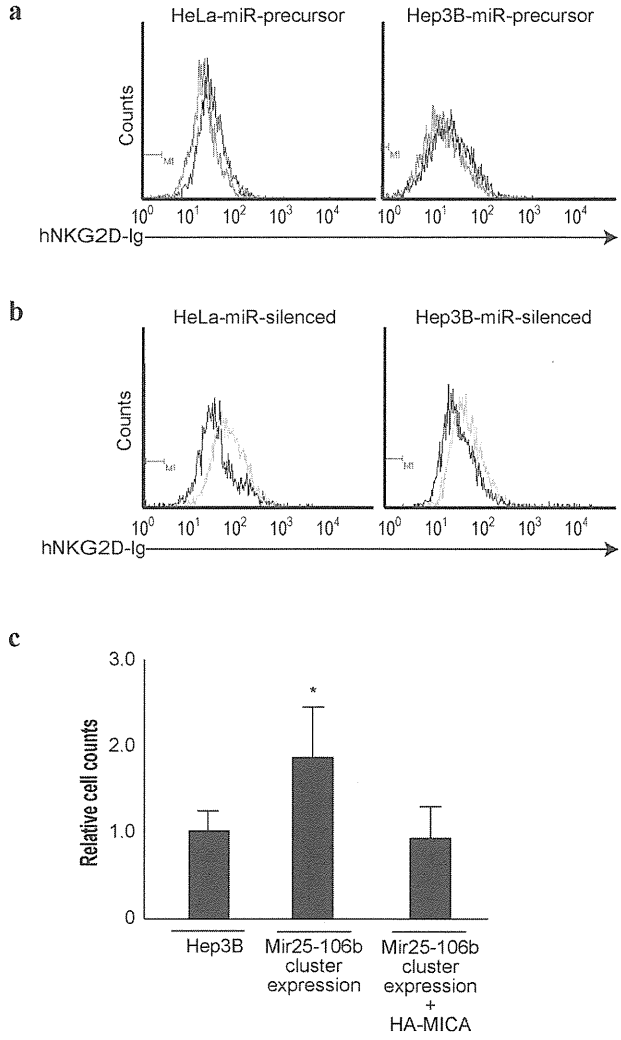

Figure 4 | NKG2D binding levels change in proportion to MICA expression levels. (a), (b), Flow cytometry of human IgG-fused NKG2D binding to the control (black lines), miR25-93-106b cluster-expressing cells (red lines) (a), and mature anti-sense sequences of miR25-93-106b cluster-expressing cells (green lines) (b). Representative results from three independent experiments are shown. (c), *In vivo* killing of DiO-labeled Hep3B and Dil-labeled HeLa cells (internal control cells) injected together into the tail veins of six mice in each group. Fluorescence intensities were quantified by flow cytometry as the ratio of Hep3B to HeLa cells in the lungs. The data from control Hep3B cells were set as 1.0. Data represent the means ± s.d. of three independent experiments. $*p < 0.05$.

dependent on miRNAs. In addition, in cells with no endogenous MICA expression, such as Huh7 cells, modulation of microRNA expression had no effect on the regulation of MICA expression. This suggests that at least low-level endogenous expression, which may be determined by promoter activities, are needed for regulation by miRNA. Therefore, changes in promoter activities and epigenetic changes in the MICA gene should also be determined. This will facilitate application of the regulatory function of miRNAs reported here.

One class of antisense oligonucleotides, namely locked nucleic acids, can be used to sequester microRNAs in the liver of various animals, including humans[16,24,25]. A clinical trial targeting miR-122 with the anti-miR-122 oligonucleotides miravirsen, the first miRNA-targeted drug, is underway for the treatment of HCV infection[16]. Thus, nucleic-acid-mediated gene therapy is becoming a realistic option. Modulation of MICA expression levels by such nucleic-acid-mediated therapy based on the results presented herein may also be a promising option for prevention and/or therapy of HCC.

In summary, we have shown that the miR25-93-106b cluster can be used to modulate MICA expression levels in HCC cells. Based on our GWAS results and associated studies, regulation of MICA protein expression levels is crucial to prevent the development of HCC during chronic hepatitis viral infection. It is important to identify the other factors that regulate MICA transcriptional activities as well as the post-translational processes and their association with susceptibility to HCCs. That said, miRNA regulation of MICA expression as shown here may facilitate regulation of the host innate immune system in an HCC-suppressive manner during chronic hepatitis viral infection.

Methods

Cell culture. The human HCC cell lines Huh7, HLE, PLC/PRF/5, and Hep3B were obtained from the Japanese Collection of Research Bioresources (JCRB, Osaka, Japan). The human cervical cancer cell line HeLa was obtained from the American Type Culture Collection (ATCC, Rockville, MD). All cells were maintained in Dulbecco's modified Eagle's medium supplemented with 10% fetal bovine serum.

Mouse. Experimental protocols were approved by the Ethics Committee for Animal Experimentation at the Graduate School of Medicine, the University of Tokyo and the Institute for Adult Disease, Asahi Life Foundation, Japan and conducted in accordance with the Guidelines for the Care and Use of Laboratory Animals of the Department of Medicine, the University of Tokyo, and the Institute for Adult Disease, Asahi Life Foundation.

Flow cytometry. Cells were hybridized with anti-MICA (1 : 500; R&D Systems, Minneapolis, MN) and isotype control IgG (1 : 500; R&D Systems) in 5% BSA/1% sodium azide/PBS for 1 h at 4°C. After washing, cells were incubated with goat anti-mouse Alexa 488 (1 : 1000; Molecular Probes, Eugene, OR) for 30 min. Flow cytometry was performed and data analyzed using Guava Easy Cyte Plus (GE Healthcare, Little Chalfont, UK).

Reporter plasmid construction, transient transfections, and luciferase assays. The reporter plasmid for the analysis of the effects of miRNAs on MICA 3′UTR were constructed by subcloning the MICA 3′UTR sequences from pLightSwitch-MICA 3UTR (SwitchGear Genomics, Menlo Park, CA) into the pGL4.50 vector (Promega, Madison, WI) at the *Fse*I site by the In-Fusion method (Clontech, Mountain View, CA) to insert the MICA 3′UTR sequences into the 3′-UTR of the firefly luciferase gene, which was under the control of the CMV promoter. The sequences of the primers were 5′-CTA GAG TCG GGG CGG CG GCC ATT TCA GCC TCT GAT GTC AGC-3′ and 5′-GTC TGC TCG AAG CGG CCG GCC TGG CCT GAG ACT CTG TCT TAA-3′. The resultant plasmid (Luc-MICA 3′UTRwt) was used as a template for the construction of mutant reporter plasmid (Luc-MICA 3′UTRmut), which carries three point mutations in the seed sequences of miR93 and 106b in the MICA 3′UTR, itself generated by a Quik Change II XL Site-directed Mutagenesis Kit (Stratagene, Heidelberg, Germany) according to the manufacturer's instructions. Transient transfection and reporter assays were performed as described previously[26].

Lentiviral constructs, viral production, and transduction. To generate a neomycin-resistant miR25-93-106b cluster-expressing lentiviral construct, copGFP in the pmiRNA25-93-106b cluster-expressing plasmid (System Biosciences, Mountain View, CA) was replaced with a neomycin resistant gene, which was subcloned from the pCDH-Neo vector (System Biosciences), at the *Fse*I site. The primers used were 5′-GCT ACC GCT ACG AGG CCG GCC CAT GAT TGA ACA AGA TGG ATT GCA-3′ and 5′-TCG CCG ATC ACG CGG CCG GCC TCA GAA GAA CTC GTC AAG AAG GC-3′. To remove the copGFP region from pmiRZIP25-93-106b (System Biosciences), a construct expressing mature anti-sense sequences of the miR25-93-106b cluster, sequences coding the GFP gene were removed by excision with *Xba*I and *Pst*I sites followed by connecting the cut ends with annealed oligonucleotides (5′-CTA GAC GCC ACC ATG CTG CA-3′ and 5′-GCA TGG TGG CGT-3′) to maintain the coding frame and the expression of the downstream puromycin-resistance gene. To generate HA-tagged MICA protein overexpressing the lentiviral construct, MICA cDNA was amplified by PCR using a Halo-tag-MICA–expressing plasmid (Promega, Madison, WI) as a template and cloned into a pCDH-puro vector (System Biosciences) at the *Not*I site. The primer sequences used were 5′-ATC GGA TCC GCG GCC GCA CCA TGT ACC CAT ACG ATG TTC CAG ATT ACG CTA TGG GGC TGG GCC CGG TC-3′ and 5′-AGA TCC TTC GCG GCC GCT TAG GCG CCC TCA GTG GAG C-3′. Let-7g precursor expressing plasmid was generated by inserting about 1,000 bp long PCR product around the let-7g genomic region into pCDH-puro vector using *Xba*1 and *Not*1 sites. The production and concentration of lentiviral particles were described previously[27]. shRNA against MICA-producing lentiviral particles with puromycin resistant gene were purchased from SantaCruz Biotechnology (sc-4924-V, Dallas, TX). Cells were transduced with lentiviruses using

polybrene (EMD Millipore, Billerica, MA). The selections were performed with 400 μg/mL G418 and 2 μg/mL (HeLa) or 6 μg/mL (Hep3B) puromycin.

Immunocytochemistry. Cells on two-well chamber slides were fixed with 4% paraformaldehyde. Fixed cells were probed with the primary MICA antibody (R&D Systems) for 1 h after blocking with 5% normal goat serum for 30 min. Cells probed with the MICA antibody were incubated with the secondary Alexa Fluor 488 goat anti-mouse antibody (Molecular Probes) for 30 min. Slides were mounted using VectaShield with DAPI (Vector Labs, Burlingame, CA).

Northern blotting of miRNAs. Northern blotting of miRNAs was performed as described previously[27]. Briefly, total RNA was extracted using TRIzol Reagent (Invitrogen, Carlsbad, CA) according to the manufacturer's instructions. Ten micrograms of RNA were resolved in denaturing 15% polyacrylamide gels containing 7 M urea in 1 × TBE and then transferred to a Hybond N+ membrane (GE Healthcare) in 0.25 × TBE. Membranes were UV-crosslinked and prehybridized in hybridization buffer. Hybridization was performed overnight at 42°C in ULTRAhyb-Oligo Buffer (Ambion) containing a biotinylated probe specific for miR93 (cta cct gca cga aca gca ctt tg) and 106b (atc tgc act gtc agc act tta), which had previously been heated to 95°C for 2 min. Membranes were washed at 42°C in 2 × SSC containing 0.1% SDS, and the bound probe was visualized using a BrightStar BioDetect Kit (Ambion). Blots were stripped by boiling in a solution containing 0.1% SDS and 5 mM EDTA for 10 min prior to rehybridization with a U6 probe (cac gaa ttt gcg tgt cat cct t).

miRNA library screening. To screen for miRNAs that target MICA 3′-UTR, synthetic miRNA mimics and reporter constructs were used as described previously[19,20]. Seventy-six types of synthetic mature miRNAs that are highly expressed in the liver[28] were custom-made (B-Bridge, Tokyo, Japan) and transfected by RNAi Max (Life Technologies, Carlsbad, CA) into Huh7 cells in 96-well plates that had been transfected 24 h before with Luc-MICA 3′UTRwt. The cells were then incubated for another 24 h. As negative controls, oligonucleotides of artificial sequences were applied[19]. The luciferase activities were measured using a GloMax 96 Microplate Luminometer (Promega). The experiments were performed in duplicate.

NKG2D binding assay. Cells were incubated with 4 μg of recombinant human NKG2D fused to human IgG1 Fc chimera protein. After washing, cells were incubated with an Alexa488-conjugated affinity purified F(ab')2 fragment of goat anti-human IgG (Jackson ImmunoResearch Laboratories, West Grove, PA). As a negative control, cells were incubated with only Alexa488 anti-human IgG. The intensity of the fluorescence was determined by flow cytometry.

***In vivo* cell-killing assay.** Hep3B cells and HeLa cells were labeled with the fluorescent dye VybrantDiO and Dil (Molecular Probes), respectively. Cells were mixed at a density of 2×10^7 in 1-ml PBS, and 200 μl was injected into the tail vein. Five hours later, lungs were collected, and single-cell suspensions were collected using a cell strainer. Fluorescence was assayed by flow cytometry, and the ratio of the experimental Hep3B cells to HeLa cells (internal control) was calculated.

Statistical analysis. Statistically significant differences between groups were determined using Student's *t*-test when variances were equal. When variances were unequal, Welch's *t*-test was used instead. *P*-values of < 0.05 were considered to indicate statistical significance.

1. El-Serag, H. B. Epidemiology of viral hepatitis and hepatocellular carcinoma. *Gastroenterology* **142**, 1264–1273 (2012).
2. Sherman, M. Hepatocellular carcinoma: New and emerging risks. *Dig Liver Dis* **42**, S215–222 (2010).
3. Arzumanyan, A., Reis, H. M. & Feitelson, M. A. Pathogenic mechanisms in HBV- and HCV-associated hepatocellular carcinoma. *Nat Rev Cancer* **13**, 123–135 (2013).
4. Urabe, Y. *et al.* A genome-wide association study of HCV-induced liver cirrhosis in the Japanese population identifies novel susceptibility loci at the MHC region. *J Hepatol* (2013).
5. Kumar, V. *et al.* Genome-wide association study identifies a susceptibility locus for HCV-induced hepatocellular carcinoma. *Nat Genet* **43**, 455–458 (2011).
6. Kumar, V. *et al.* Soluble MICA and a MICA variation as possible prognostic biomarkers for HBV-induced hepatocellular carcinoma. *PLoS One* **7**, e44743 (2012).
7. Maccalli, C., Scaramuzza, S. & Parmiani, G. TNK cells (NKG2D+ CD8+ or CD4+ T lymphocytes) in the control of human tumors. *Cancer Immunol Immunother* **58**, 801–808 (2009).
8. Jinushi, M. *et al.* Impairment of natural killer cell and dendritic cell functions by the soluble form of MHC class I-related chain A in advanced human hepatocellular carcinomas. *J Hepatol* **43**, 1013–1020 (2005).
9. Diefenbach, A., Jensen, E. R., Jamieson, A. M. & Raulet, D. H. Rae1 and H60 ligands of the NKG2D receptor stimulate tumour immunity. *Nature* **413**, 165–171 (2001).
10. Hayakawa, Y. Targeting NKG2D in tumor surveillance. *Expert Opin Ther Targets* **16**, 587–599 (2012).
11. Guerra, N. *et al.* NKG2D-deficient mice are defective in tumor surveillance in models of spontaneous malignancy. *Immunity* **28**, 571–580 (2008).
12. Bauer, S. *et al.* Activation of NK cells and T cells by NKG2D, a receptor for stress-inducible MICA. *Science* **285**, 727–729 (1999).
13. Eleme, K. *et al.* Cell surface organization of stress-inducible proteins ULBP and MICA that stimulate human NK cells and T cells via NKG2D. *J Exp Med* **199**, 1005–1010 (2004).
14. Yadav, D., Ngolab, J., Lim, R. S., Krishnamurthy, S. & Bui, J. D. Cutting edge: down-regulation of MHC class I-related chain A on tumor cells by IFN-gamma-induced microRNA. *J Immunol* **182**, 39–43 (2009).
15. Stern-Ginossar, N. & Mandelboim, O. An integrated view of the regulation of NKG2D ligands. *Immunology* **128**, 1–6 (2009).
16. Janssen, H. L. *et al.* Treatment of HCV Infection by Targeting MicroRNA. *N Engl J Med* **368**, 1685–94 (2013).
17. Salih, H. R., Rammensee, H. G. & Steinle, A. Cutting edge: down-regulation of MICA on human tumors by proteolytic shedding. *J Immunol* **169**, 4098–4102 (2002).
18. Tang, K. F. *et al.* Decreased Dicer expression elicits DNA damage and up-regulation of MICA and MICB. *J Cell Biol* **182**, 233–239 (2008).
19. Takata, A. *et al.* MicroRNA-22 and microRNA-140 suppress NF-κB activity by regulating the expression of NF-κB coactivators. *Biochem Biophys Res Commun* **411**, 826–831 (2011).
20. Yoshikawa, T. *et al.* Silencing of microRNA-122 enhances interferon-a signaling in the liver through regulating SOCS3 promoter methylation. *Sci. Rep.* **2**, 637 (2012).
21. Lewis, B. P., Burge, C. B. & Bartel, D. P. Conserved seed pairing, often flanked by adenosines, indicates that thousands of human genes are microRNA targets. *Cell* **120**, 15–20 (2005).
22. Gazit, R. *et al.* Lethal influenza infection in the absence of the natural killer cell receptor gene Ncr1. *Nat Immunol* **7**, 517–523 (2006).
23. Lo, P. H. *et al.* Identification of a Functional Variant in the MICA Promoter Which Regulates MICA Expression and Increases HCV-Related Hepatocellular Carcinoma Risk. *PLoS One* **8**, e61279 (2013).
24. Lanford, R. E. *et al.* Therapeutic silencing of microRNA-122 in primates with chronic hepatitis C virus infection. *Science* **327**, 198–201 (2010).
25. Elmén, J. *et al.* LNA-mediated microRNA silencing in non-human primates. *Nature* **452**, 896–899 (2008).
26. Kojima, K. *et al.* MicroRNA122 is a key regulator of α-fetoprotein expression and influences the aggressiveness of hepatocellular carcinoma. *Nat Commun* **2**, 338 (2011).
27. Takata, A. *et al.* MicroRNA-140 acts as a liver tumor suppressor by controlling NF-κB activity by directly targeting DNA methyltransferase 1 (Dnmt1) expression. *Hepatology* **57**, 162–170 (2013).
28. Krützfeldt, J. *et al.* Silencing of microRNAs in vivo with 'antagomirs'. *Nature* **438**, 685–689 (2005).

Acknowledgments

This work was supported by Grants-in-Aid from the Ministry of Education, Culture, Sports, Science and Technology, Japan (#25293076, #25460979, and #24390183) (to M.Otsuka, Y.K. and K.K.), by Health Sciences Research Grants of The Ministry of Health, Labour and Welfare of Japan (to K.K.), and by grants from the Okinaka Memorial Institute for Medical Research, the Liver Forum in Kyoto, and the Princess Takamatsu Cancer Research Fund (to M.Otsuka).

Author contributions

T.K., M. Otsuka and K.K. planned the research and wrote the paper. T.K., M. Otsuka, T.Y., M. Ohno, A.T., C.S. and Y.K. performed the majority of the experiments. M.A. and H.Y. supported several experiments and analyzed the data. K.K. supervised the entire project.

Additional information

Supplementary information accompanies this paper at http://www.nature.com/scientificreports

Competing financial interests: The authors declare no competing financial interests.

How to cite this article: Kishikawa, T. *et al.* Regulation of the expression of the liver cancer susceptibility gene MICA by microRNAs. *Sci. Rep.* 3, 2739; DOI:10.1038/srep02739 (2013).

SCIENTIFIC REPORTS

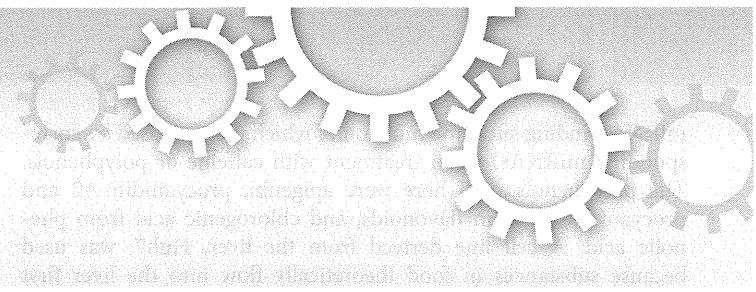

OPEN

SUBJECT AREAS:
MIRNAS
NUTRIENT SIGNALLING
NATURAL PRODUCTS
TYPE 2 DIABETES MELLITUS

Received
10 May 2013

Accepted
15 August 2013

Published
30 August 2013

Correspondence and requests for materials should be addressed to M.O. (otsukamo-tky@umin.ac.jp)

* These authors contributed equally to this work.

The flavonoid apigenin improves glucose tolerance through inhibition of microRNA maturation in miRNA103 transgenic mice

Motoko Ohno[1]*, Chikako Shibata[1]*, Takahiro Kishikawa[1], Takeshi Yoshikawa[1], Akemi Takata[1], Kentaro Kojima[1], Masao Akanuma[2], Young Jun Kang[3], Haruhiko Yoshida[1], Motoyuki Otsuka[1,4] & Kazuhiko Koike[1]

[1]Department of Gastroenterology, Graduate School of Medicine, The University of Tokyo, Tokyo 113-8655, Japan, [2]Division of Gastroenterology, The Institute for Adult Diseases, Asahi Life Foundation, Tokyo 100-0005, Japan, [3]Department of Immunology and Microbial Sciences, The Scripps Research Institute, La Jolla, CA 92037, USA, [4]Japan Science and Technology Agency, PRESTO, Kawaguchi, Saitama 332-0012, Japan.

Polyphenols are representative bioactive substances with diverse biological effects. Here, we show that apigenin, a flavonoid, has suppressive effects on microRNA (miRNA) function. The effects were mediated by impaired maturation of a subset of miRNAs, probably through inhibition of the phosphorylation of TRBP, a component of miRNA-generating complexes via impaired mitogen-activated protein kinase (MAPK) Erk activation. While glucose intolerance was observed in miRNA103 (miR103)-overexpressing transgenic mice, administration of apigenin improved this pathogenic status likely through suppression of matured miR103 expression levels. These results suggest that apigenin may have favorable effects on the pathogenic status induced by overexpression of miRNA103, whose maturation is mediated by phosphorylated TRBP.

Polyphenols, common components of many popular drinks and foods, and caffeine, an alkaloid in various seeds and leaves, are representative bioactive substances with diverse biological effects[1,2]. However, while some effects have been examined in detail[3], the molecular mechanisms underlining these biological effects are mostly undetermined.

MicroRNAs (miRNAs) are short, single-stranded, non-coding RNAs expressed in most organisms ranging from plants to vertebrates[4]. Primary miRNAs, which possess stem-loop structures, are processed into mature miRNAs by Drosha, Dicer, RNA polymerase III, and other related molecules. These mature miRNAs then bind the RNA-induced silencing complex (RISC), and the resulting co-complex directly binds the 3′-untranslated regions (3′-UTRs) of target mRNAs to act as suppressors of translation and gene expression. Thus, dependent upon the identity of the target mRNAs, miRNAs are responsible for the control of various biological functions, including cell proliferation, apoptosis, differentiation, metabolism, oncogenesis, and oncogenic suppression[5–9]. For example, it was reported recently that expression of miRNA103 and 107 (miR103 and 107) was upregulated in obese mice, and that the gain of miR103 function in either liver or fat was sufficient to induce impaired glucose homeostasis[10].

Because the effects of bioactive substances are diverse and the functions of miRNAs result in diverse biological consequences, we hypothesized that some effects of bioactive substances may depend on modulation of miRNA function. In this study, we examined whether polyphenols and caffeine affect miRNA function and determined the molecular mechanisms underlying these effects. In addition, we applied the results obtained here to clinically relevant models to facilitate their use in practical applications.

Results

Apigenin suppresses miRNA function. To determine the effects of polyphenols and caffeine on miRNA function, we determined the luciferase activities of several types of reporters constructed containing

miRNA-binding sites (the function of which is suppressed by corresponding miRNAs) upon treatment with caffeine or polyphenols. The polyphenols used here were apigenin, procyanidin A2 and procyanidin B2 from flavonoids, and chlorogenic acid from phenolic acid. A cell line derived from the liver, Huh7, was used because substances in food theoretically flow into the liver first through the portal vein immediately after intestinal absorption. Among the bioactive substances examined, only apigenin significantly inhibited the effects of miRNAs such as miR122, miR185 and miR103 (Figure 1a), which are highly expressed in the liver[11]. The effects were similarly observed irrespective of endogenous miRNAs or exogenous overexpression of corresponding miRNAs (Figure 1a and b) in a dose-dependent manner (Figure 1c). Another liver cell line, Hep3B, showed similar results, suggesting that the effects were not cell line-specific (Supplementary Figure 1a, b and c). The effects were detected with 5 μM apigenin; this concentration is physiologically attainable[12–14]. These results suggest that apigenin has suppressive effects on miRNA function.

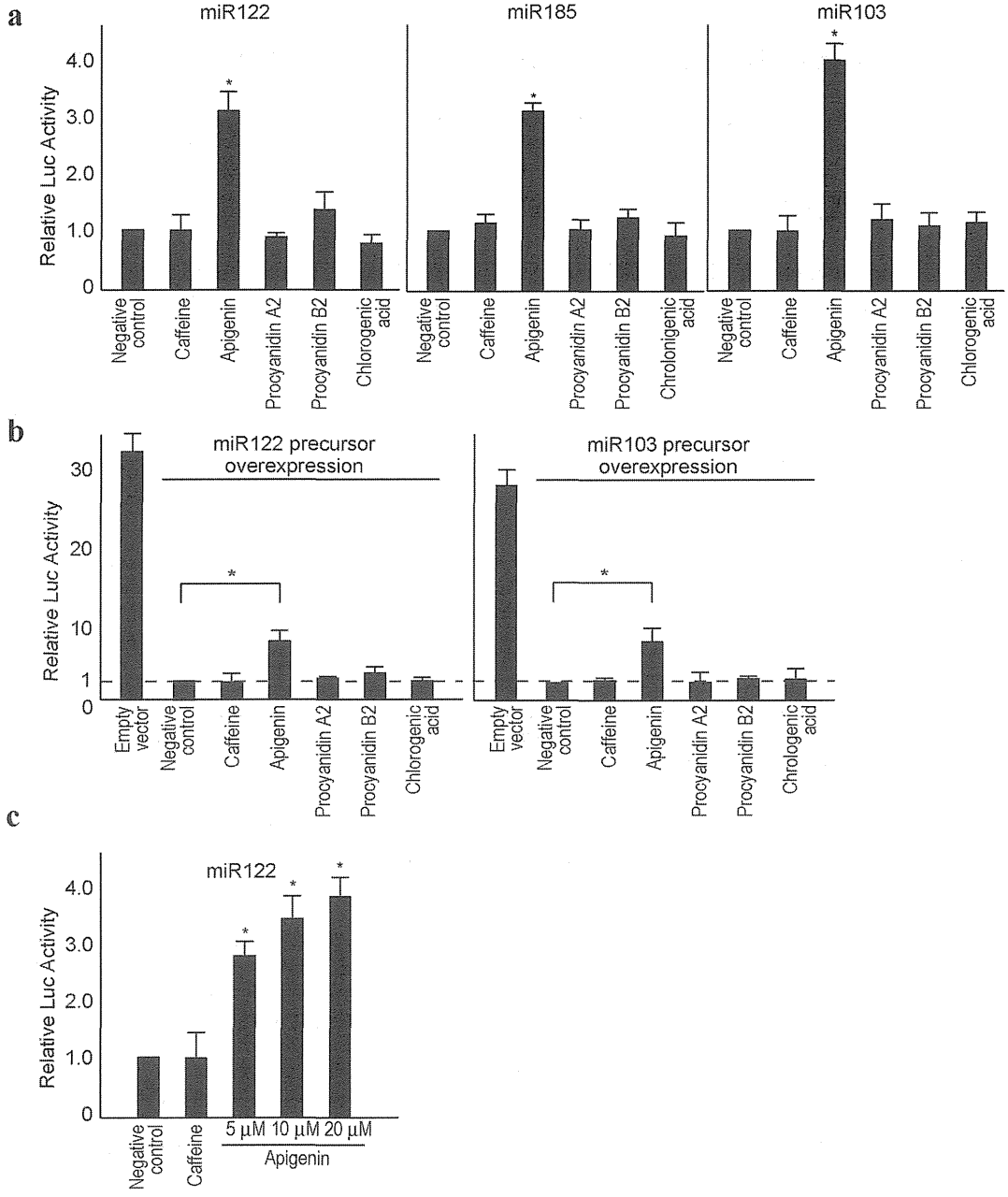

Figure 1 | Apigenin inhibits miRNA function. (a), Apigenin inhibits endogenous miRNA function. Huh7 cells were transfected with reporters to determine the functions of the indicated miRNAs. Twenty-four hours after treatment with the indicated substances, reporter assays were performed. Data represent the means ± standard deviation (s.d.) from three independent experiments. *, $p < 0.05$ (*t*-test). (b), Apigenin inhibits the function of exogenously overexpressed miRNAs. Huh7 cells were transfected with reporters and corresponding miRNA precursor-expressing plasmids or an empty vector. Twenty-four hours after treatment with the indicated substances, reporter assays were performed. Data represent the means ± s.d. from three independent experiments. *, $p < 0.05$ (*t*-test). (c), Dose-dependent effects of apigenin on miRNA function. Huh7 cells were transfected with reporter plasmids to determine miR122 function. Cells were treated with indicated doses of apigenin for 24 h and luciferase assays were performed. Caffeine was included as a negative control. Data represent the means ± s.d. from three independent experiments. *, $p < 0.05$ (*t*-test) compared with the negative control.

Apigenin inhibits miRNA maturation from miRNA precursors. To elucidate the molecular mechanisms underlying the inhibitory effects of apigenin on miRNA function, we first determined the expression levels of miRNA pathway-related molecules including Drosha, DGCR8, KSRP, Argonaute 2 (Ago2), and Dicer in the presence of apigenin. While the expression levels of Drosha, Ago2 and Dicer proteins appeared to decrease slightly after a high dose of apigenin, no significant changes were observed in the expression levels of these proteins (Figure 2a and Supplementary Figure 2a). Next, we examined the expression and maturation of miRNAs by quantitative real-time polymerase chain reaction (qRT-PCR) and Northern blotting (Figure 2b and Supplementary Figure 2b). Expression levels of mature endogenous miR122, miR103, and miR185 decreased and accumulation of precursor miRNAs was also observed after apigenin treatment (Figure 2b), suggesting that maturation from miRNA precursors was decreased. In addition, a comprehensive miRNA microarray analysis confirmed that apigenin altered the expression levels of a major subset of miRNAs (Supplementary Figure 2c; the raw data were deposited in the GEO database; GSE46526). However, some miRNAs, such as let-7, were not affected by apigenin treatment, which was confirmed by qRT-PCR (Figure 2b). These results suggest that apigenin has an inhibitory effect on the maturation of a subset of miRNAs.

Apigenin inhibits phosphorylation of TRBP. The microRNA-generating complex is composed of Dicer and phospho-TRBP isoforms[15], and TRBP phosphorylation enhances the maturation of a subset of miRNAs through stabilization of the microRNA-generating complexes[15]. Phosphorylation of TRBP is mediated by mitogen-activated protein kinase (MAPK) Erk[15]. Because apigenin is known to inhibit Erk activity[16–19], we hypothesized that the inhibitory effects of apigenin on miRNA maturation may be mediated by decreased phosphorylation of TRBP through inhibition of Erk. Consistent with previous reports, although caffeine had no effect on the Erk phosphorylation status, apigenin clearly inhibited Erk phosphorylation 24 h post-treatment without changes in total Erk levels (Figure 3a). Concordantly, SRE-driven reporter activities were diminished by apigenin treatment (Figure 3b), suggesting that apigenin indeed inhibited an Erk-mediated intracellular signaling pathway, consistent with previous reports[16–19]. While TRBP was phosphorylated under normal serum culture conditions, and its phosphorylation status did not change with caffeine treatment, its phosphorylation was inhibited by apigenin (Figure 3c). This effect was confirmed by electrophoresis in a phos-tag gel, which showed a clear slow-migrating band, indicating that TRBP was phosphorylated in control and caffeine-treated conditions, but its phosphorylation was inhibited upon treatment with apigenin (Figure 3d). To confirm that Erk activity was inhibited by apigenin following TRBP phosphorylation, we examined the effects of apigenin using Huh7 cells stably expressing constitutively active Mek1 (CA-MEK) on TRBP phosphorylation. As shown in Figure 3e, the degree of TRBP phosphorylation was increased only by CA-MEK expression, and the augmented phosphorylation was not diminished by apigenin treatment (Figure 3e), suggesting that the effects of apigenin could not be observed under the induced Erk activation. That is, the effects of apigenin were most probably mediated by inhibition of Erk activation. In addition, we established Huh7 cells stably expressing dominant negative Erk (DN-Erk). As predicted, the levels of mature miRNA103, 122, and 185, were decreased in DN-Erk expressing cells, but were slightly increased in CA-MEK expressing cells, irrespective of apigenin treatment (Figure 3f). The expression levels of mature let-7, which were examined as a representative miRNA that was not affected by apigenin treatment in the miRNA microarray (Figure 3f), were not changed by enforced expression of DN-Erk or CA-MEK, suggesting that this miRNA maturation is not significantly regulated by MAPK activity or TRBP phosphorylation, consistent with a previous report[15]. These results suggest that apigenin inhibits Erk phosphorylation, and subsequent decreased MAPK activity leads to a decrease in TRBP phosphorylation, which may result in decreased maturation of a subset of miRNAs.

Apigenin improves glucose tolerance through inhibition of miRNA function. To apply the above results in a clinical setting, we focused on recent findings demonstrating that a gain of miR103/107 expression induces impaired glucose homeostasis *in vivo*[10]. To utilize this, we generated transgenic mice expressing a miR103 precursor under control of the CMV promoter (Supplementary Figure 3a). Overexpression of miR103 in these mice was confirmed by Northern blotting against mature miR103 in liver tissues (Figure 4a and Supplementary Figure 3b). No significant over-saturation of RISC

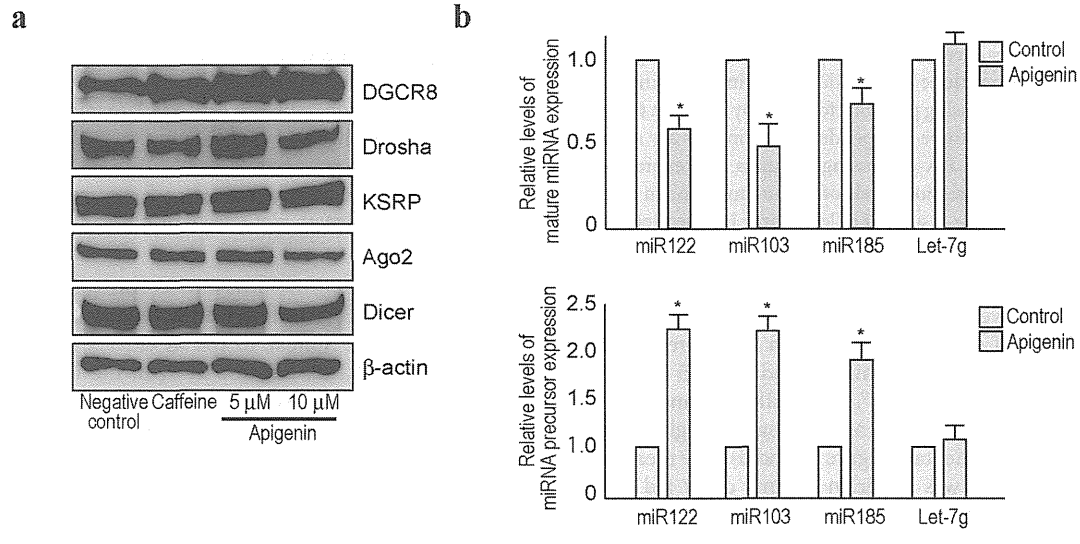

Figure 2 | Apigenin impairs miRNA maturation. (a), Cells were treated with the appropriate substances for 24 h and the indicated proteins were blotted. Representative results from three independent experiments using Huh7 cells are shown. Full-length blot images are available in Supplementary Figure 5a. (b), The expression levels of mature miRNAs and miRNA precursors were determined by qRT-PCR using Huh7 cells with or without apigenin treatment for 24 h. Data represent the means ± s.d. from three independent experiments. *, $p < 0.05$ (t-test) compared with the control (DMSO only) treatment.

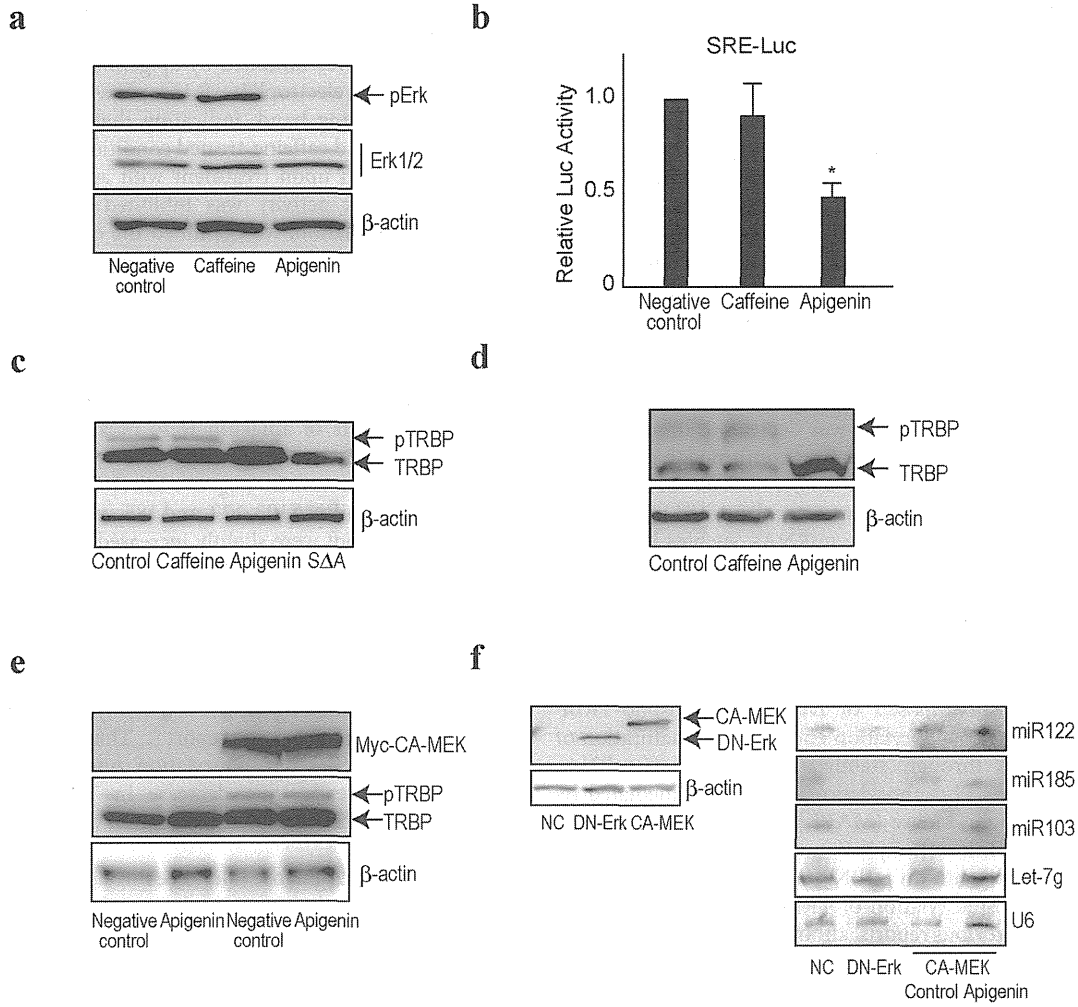

Figure 3 | Apigenin inhibits TRBP phosphorylation. (a), Cells were treated with caffeine or apigenin for 24 h. Cell lysates were blotted with anti-phosphorylated Erk and anti-total Erk1/2. Representative results from three independent experiments using Huh7 cells are shown. Similar results were obtained using Hep3B cells. (b), A luciferase assay was performed to determine SRE-driven transcription under apigenin treatment. Caffeine was included as a comparison. Data represent the means ± s.d. from three independent experiments using Huh7 cells. *, $p < 0.05$ (*t*-test) compared to the negative control. (c), Huh7 cells were transfected with wild-type TRBP-expressing plasmids followed by treatment with the indicated substances for 24 h. Serine-to-alanine mutant TRBP (SΔA) indicates non-phosphorylated TRBP. Representative results from three independent experiments using Huh7 cells are shown. (d), Substance-treated Huh7 cell lysates were separated using a Mn2+-Phos-tag gel to discriminate the phosphorylated form of TRBP. Representative results from three independent experiments using Huh7 cells are shown. (e), TRBP-expressing Huh7 cells were stably transfected with myc-tagged CA-MEK-expressing plasmids followed by apigenin treatment for 24 h. Phosphorylation status of TRBP was determined by Western blotting. Representative results from three independent experiments are shown. (f), Huh7 cells were stably transfected with myc-tagged CA-MEK-expressing plasmids or myc-tagged DN-Erk-expressing plasmids. The expression of the transfected constructs was confirmed by Western blotting using anti-myc antibodies (left panels). Expression levels of mature miRNAs in those cells with or without apigenin treatment were determined by Northern blotting (right panels). Representative results of at least three independent experiments are shown. Full-length blot images in a, b, c, d, e, and f are available in Supplementary Figure 5b, c, d, e, and f.

complexes due to overexpressing miR103 in these mice was confirmed by a lack of significant changes in the expression levels of other mature miRNAs, such as miR122 and miR185 (Figure 4a). As expected from a previous report[10], these miR103 transgenic mice showed an increase in both random and fasting blood-glucose levels and insulin levels (Supplementary Figure 3c and d). The mean size of adipocytes in visceral fat was larger in normal chow fed miR103 transgenic mice than in control mice, and their size became larger nearly in parallel in both control and miR103 transgenic mice under a high-fat diet (Supplementary Figure 3e).

To determine the effect of apigenin in these models, 40 mg/kg apigenin was intraperitoneally injected daily for 14 days in miR103 transgenic mice. The level of mature miR103 was decreased, and precursors accumulated in apigenin-treated mice, as determined by Northern blotting and qRT-PCR (Figure 4b and Supplementary Figure 4a and b). Similar to the in vitro results, levels of mature miR122 and miR185, but not let-7, in the liver tissues were also decreased by apigenin treatment (Supplementary Figure 4a and b). Phosphorylated TRBP in the liver tissues was decreased in apigenin-treated mice, as determined by a retarded band in the phos-tag gel (Figure 4c), consistent with the *in vitro* results (Figure 3d). Erk phosphorylation was consistently decreased following apigenin treatment (Supplementary Figure 4c). In addition, we confirmed the upregulated expression level of caveolin-1, a major regulator of the insulin receptor, which is a direct target gene of miR103[10] in these tissues (Supplementary Figure 4c). As expected from these results, apigenin-treated miR103 transgenic mice showed decreased random and fasting blood glucose-levels (Figure 4d). While miR103 transgenic mice